Article

Bioremediation of complex organic pollutants by engineered *Vibrio natriegens*

https://doi.org/10.1038/s41586-025-08947-7

Received: 6 June 2023

Accepted: 27 March 2025

Published online: 07 May 2025

Check for updates

Cong Su[1,4], Haotian Cui[2,4], Weiwei Wang[2,4], Yong Liu[1], Zhenyu Cheng[2], Chen Wang[1], Mengqiao Yang[2], Liwen Qu[1], Ye Li[2], Yuejin Cai[3], Siyang He[2], Jiaxin Zheng[3], Pingping Zhao[3], Ping Xu[2], Junbiao Dai[1,3] ✉ & Hongzhi Tang[2] ✉

Industrial wastewater, petroleum pollution and plastic contamination are significant threats to global marine biosecurity because of their toxic, mutagenic and persistent nature[1]. The use of microorganisms in bioremediation has been constrained by the complexity of organic pollutants and limited tolerance to saline stress[2]. In this study, we used synthetic biology to engineer *Vibrio natriegens* into a strain capable of bioremediating complex organic pollutants in saline wastewater and soils. The competence master regulator gene *tfoX* was inserted into chromosome 1 of the *V. natriegens* strain Vmax and overexpressed to enhance DNA uptake and integration. Degradation gene clusters were chemically synthesized and assembled in yeast. We developed a genome engineering method (iterative natural transformation based on Vmax with amplified *tfoX* effect) to transfer five gene clusters (43 kb total) into Vmax. The engineered strain has the ability to bioremediate five organic pollutants (biphenyl, phenol, naphthalene, dibenzofuran and toluene) covering a broad substrate range, from monocyclic to multicyclic compounds, in industrial wastewater samples from a chlor–alkali plant and a petroleum refinery.

Complex organic pollutants (such as petroleum and wastewater from oil refineries) encompass polycyclic aromatic hydrocarbons (PAHs) and monoaromatic hydrocarbons. These aromatic hydrocarbons are often found as a mixture of several components that enter oceans through atmospheric deposition or crude oil leakage, presenting profound threats to human health and delicate ecosystems[3,4]. These compounds can be bioremediated by bacteria[5]. Although these bacteria typically cannot treat complex organic pollutants because they generate catabolic enzymes that are specific to a single component or a few components with similar chemical structures, the use of consortia of microbes has been demonstrated to be effective in the bioremediation of seawater or saline water polluted by complex mixtures of organic pollutants[6,7]. The growth rate and tolerance to harsh liquid or solid phases, such as high or low pH and high salinity, are also influencing factors for microorganisms involved in the remediation of industrial wastewater, saline soils, marine water and other sites[8,9]. The expanding field of synthetic biology has led to innovative approaches for developing degrading strains for bioremediation of contaminated sites[5].

Vibrio natriegens is a promising chassis species that has been used in synthetic biology[10]. It is the fastest-growing documented bacterial species that shows adequate tolerance to elevated salt and has the ability to efficiently convert diverse carbon sources to valuable bioproducts[11,12]. Several genome engineering tools have been developed for *V. natriegens*, including SWAPnDROP[13], NT-CRISPR[14] and multiplex genome editing by natural transformation[15]. This microorganism has been phenotypically and genomically characterized as a generally safe biological agent suitable for use in biotechnology[16].

Here we aimed to establish a *V. natriegens* strain capable of remediating a range of pollutants (from monocyclic benzene to bicyclic and multicyclic compounds), on the basis of the integration of several degradation gene clusters (Fig. 1a). To improve the transformation efficiency of the *V. natriegens* Vmax, we constructed a strain harbouring a foreign *tfoX* gene on chromosome (chr.) 1. Subsequently, nine degradation gene clusters were synthesized in vitro, assembled in yeast and integrated into the Vmax genome to generate candidate strains capable of remediating the targeted pollutants. Five gene clusters were selected from a pool of candidate strains according to their remediation performance. We developed the iterative natural transformation based on Vmax with amplified *tfoX* effect (INTIMATE) method and integrated all five degradation gene clusters into a final chassis strain. We then evaluated the resulting strain for simultaneous remediation of five organic pollutants in seawater, industrial wastewater and saline soil.

Selection of chassis strains

We initially explored the use of *V. natriegens* Vmax as a chassis cell for remediation of organic pollutants, similar to several well-established species for (*P. putida* KT2440, *Sphingomonas* sp. SHPJ-2 and *B. xenovorans* LB400) (Supplementary Table 1). We compared the growth ability of Vmax with these species in various media: lysogeny broth (LB), $LB_{1/4}$ (LB with 0.25 × 10.0 g l^{-1} NaCl), LB_3 (LB with 3 × 10.0 g l^{-1} NaCl),

[1]Shenzhen Key Laboratory of Synthetic Genomics, Guangdong Provincial Key Laboratory of Synthetic Genomics, Shenzhen Institute of Synthetic Biology, Shenzhen Institutes of Advanced Technology, Chinese Academy of Sciences, Shenzhen, China. [2]State Key Laboratory of Microbial Metabolism, and School of Life Sciences & Biotechnology, Shanghai Jiao Tong University, Shanghai, People's Republic of China. [3]Shenzhen Branch, Guangdong Laboratory for Lingnan Modern Agriculture, Shenzhen Key Laboratory of Agricultural Synthetic Biology, Genome Analysis Laboratory of the Ministry of Agriculture and Rural Affairs, Agricultural Genomics Institute at Shenzhen, Chinese Academy of Agricultural Sciences, Shenzhen, China. [4]These authors contributed equally: Cong Su, Haotian Cui, Weiwei Wang. ✉e-mail: daijunbiao@caas.cn; tanghongzhi@sjtu.edu.cn

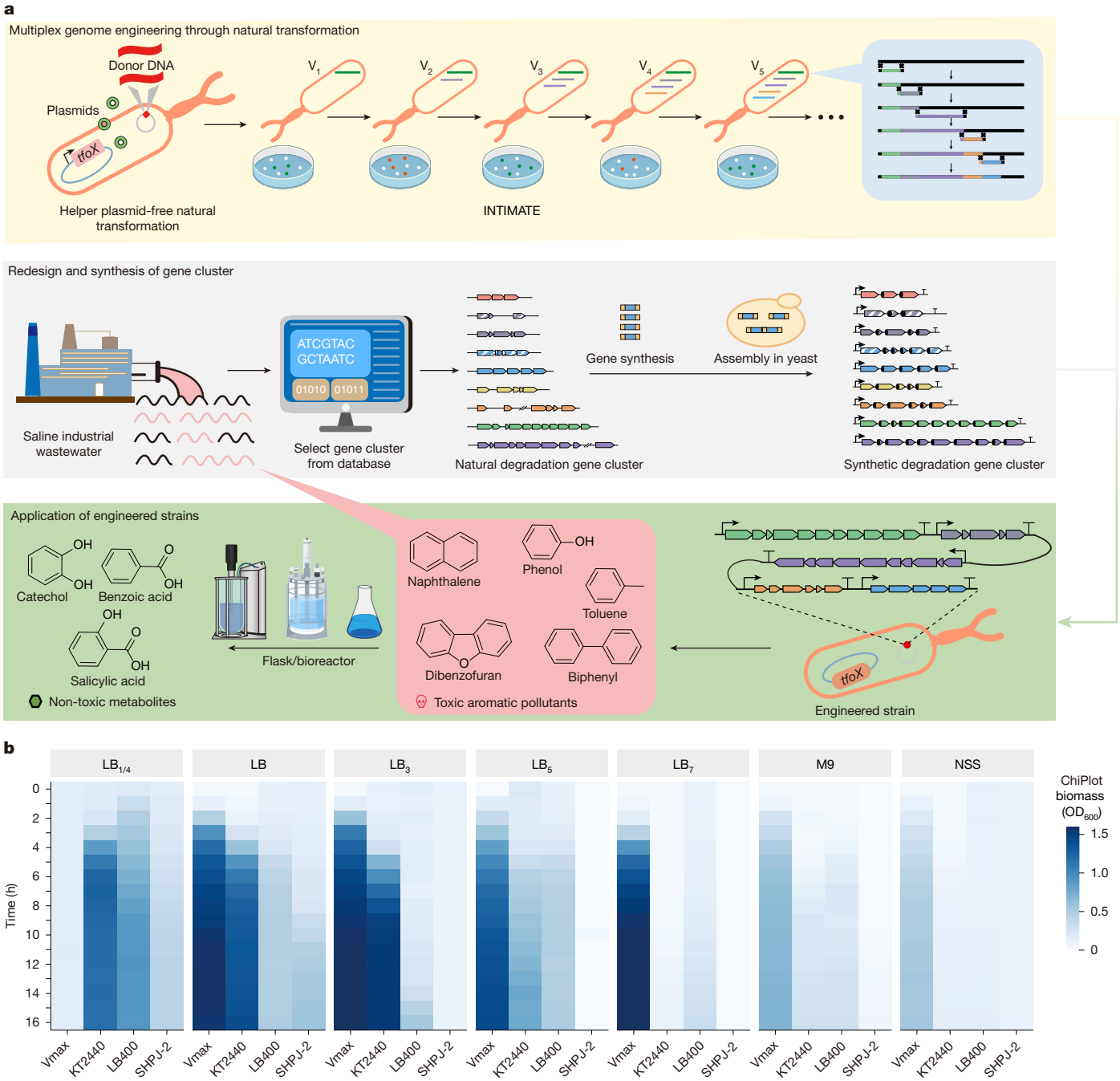

Fig. 1 | Construction of strains for remediation of complex organic pollutants and selection of chassis cells. a, Schematic summarizing the development of strains for remediation of complex organic pollutants. A complex pollutant remediation strain was developed using the 'design–building–testing–learning' strategy. During the design stage, the degradation gene clusters for monoaromatic hydrocarbons (benzene, toluene and phenol) and PAHs (biphenyl, naphthalene, DBF and DBT) were synthesized and then assembled in yeast. During the building stage, the gene clusters were inserted into the genome of the chassis cells. We inserted *tfoX* from *Vibrio cholerae* into the genome of *V. natriegens* Vmax to amplify its efficiency in natural transformation. An iterative natural transformation method known as INTIMATE was developed to insert all gene clusters into the genome of Vmax and generate remediation strains. During the testing stage, the remediation strains were exposed to seawater and industrial wastewater containing pollutants and tested to monitor the transformation of pollutants into harmless substances in flasks, activated sludge bioreactors and multi-parallel bioreactors. During the learning stage, functional gene clusters characterized as effective were concatenated and inserted into a single chassis cell to generate a complex organic pollutant remediation strain. **b**, Biomass (OD_{600}) of *V. natriegens* Vmax, *Pseudomonas putida* KT2440, *Burkholderia xenovorans* LB400 and *Sphingomonas* sp. SHPJ-2 in different media. The grey bars above the grids indicate seven media in which the strains were cultured: media containing tryptone and yeast extract as carbon and nitrogen sources with different salinities ($LB_{1/4}$, LB, LB_3, LB_5 and LB_7) and two saline solutions added with glycerol and NH_4Cl as sole nitrogen and carbon source (M9 and NSS). The colours in each cell in the grids indicate the biomass (OD_{600}) of the strains after 16 h. All data were derived from Supplementary Fig. 1. Panel **a** was created using BioRender (https://biorender.com).

LB_5 (LB with 5 × 10.0 g l^{-1} NaCl), LB_7 (LB with 7 × 10.0 g l^{-1} NaCl), M9 (minimal medium with glycerol) and nine-salt solution (NSS) with glycerol[17] medium (Supplementary Table 2). Although Vmax exhibited no remarkable performance against KT2440 and LB400 under the saline-deficient condition, it had a higher final biomass than the other strains at optical density at 600 nm (OD_{600}) of 1.4 in LB_3, LB_5

and LB_7 media. In addition, it grew in NSS and M9 media, reaching an OD_{600} value of 0.5 after 16 h (Fig. 1b and Supplementary Fig. 1). After including organic pollutants, such as biphenyl, phenol, naphthalene, dibenzofuran (DBF) and toluene, in the $LB_{1/4}$, LB, LB_3 and LB_5 media, we compared the growth rates of these species. In the saline-deficient $LB_{1/4}$ medium, KT2440 and LB400 exhibited faster growth rates. When the salt concentration in the medium reached 30.0 or even 50.0 g l^{-1}, Vmax demonstrated a superior growth rate than the others under a detected concentration of organic pollutants (Fig. 2a and Supplementary Figs. 2–5). This suggests that Vmax exhibited tolerance to pollutants in high-salt environments.

The outstanding tolerance of Vmax towards organic pollutants piqued our interest in exploring the associated potential genes and metabolic pathways. We profiled transcriptome changes in Vmax under the stress of complex organic pollutants (biphenyl, phenol, naphthalene, DBF and toluene). Of the 57 annotated ABC transporters, 43 were reported to consist of membrane transporters for organic pollutants[18] and detected as being upregulated. Under the stress of complex organic pollutants, the transcription levels of the genes of global transcription factors (*fleQ*, *marA*, *pcaQ*, *pyrl* and *ysmB*), multiple drug resistance proteins (mdtA and mdtN) and channel proteins located in the outer membrane (acrA, acrB, bepG, czcA, fadL, tolC, vmeY, vmeZ, ybaR and yicG) were significantly increased (Extended Data Fig. 1a). We specifically noticed the upregulated transcriptional levels of *marA* and acrAB–tolC, which serve as efflux pumps in gram-negative strains[19]. The transcriptional level of *marA*, acrA, acrB and tolC was upregulated for 1.7-, 3.5-, 3.3- and 2.5-folds in Vmax cultured under the stress of pollutants (Extended Data Fig. 1b).

Generating an optimized VCOD-2 strain

For highly efficient transformation and protein expression, approximately 150 genes were deleted from *V. natriegens* Vmax[20]. Promoter functions have not been thoroughly investigated in Vmax but have been completed in wild-type *V. natriegens*[21]. Therefore, we used sfGFP reporter expression assays in the Vmax chassis strain to examine the activity of constitutive promoters and inducible promoters: P_{lac}, P_c, P_{J23110}, P_{lambda}, P_{tac}, P_{J23119}, P_{25}, P_{T7} (induced by isopropyl β-D-1-thiogalactopyranoside (IPTG)) and P_{BAD} (induced by arabinose) (Supplementary Table 3). Ultimately, the constitutive P_{25} and inducible P_{T7} promoters demonstrated superior strength among them, chosen to drive gene transcription in Vmax (Supplementary Fig. 6).

V. natriegens has potential genes associated with natural transformation, and its expression is enhanced by the global transcription factor *tfoX*[15]. This expression facilitates the uptake of exogenous transforming DNA into cells and its subsequent integration into the genome (Supplementary Fig. 7). We transformed pET28a-*tfoX* into Vmax to generate a new strain (VCOD-1), which has the capacity for natural transformation. After inducing *tfoX*, we examined the ability of VCOD-1 to absorb exogenous DNA. We chose the *wbfF* gene, which enables the production of a capsular polysaccharide, to evaluate the transformation efficiency. Deleting *wbfF* resulted in the production of opaque Vmax colonies when grown on agar plates, allowing visual assessment of transformants. The efficiency of natural transformation in Vmax was aligned with previously reported efficiencies in this bacterium (Extended Data Fig. 2).

Examination of the whole-genome sequencing of Vmax demonstrated that the gene encoding the Dns exonuclease on Vmax chr. 1 was replaced by a T7 RNA polymerase expression box (encompassing a Lac repressor, β-galactosidase, RNA polymerase, integrase and Loxp66/77). We chose the integrase gene site (*int*) downstream of T7 RNA polymerase and used natural transformation to insert donor DNA containing *tfoX* under the control of the T7 promoter and p15A plasmid (possessing a chloramphenicol resistance marker) into VCOD-1 (Fig. 2b). Following the loss of pET28a-*tfoX* and p15A plasmid through continuous culturing, we obtained VCOD-2 containing *tfoX* integrated into chr. 1 and lacking a resistance marker. We compared the efficiency of natural transformation between VCOD-2 and VCOD-1 by replacing *wbfF* with the chloramphenicol resistance marker. VCOD-2 showed improved efficiency for plasmid transformations (Fig. 2c). For linear donor transformation, VCOD-2 showed better efficiency when the usage of the donor was higher than 5 ng and the length of the donor was longer than 1 kilobase (kb) (Fig. 2d,e). The growth of VCOD-2 was not reduced compared to Vmax (Fig. 2f). Therefore, we considered VCOD-2 to be a suitable chassis for a variety of molecular biology and biotechnology applications. We further optimized the natural transformation experimental parameters in VCOD-2 to maximize the transformation efficiency (Extended Data Fig. 3) and optimized VCOD-2 to be suitable as a chassis for a variety of molecular biology and biotechnology applications.

Screening an insertion site

To achieve a stable and homogeneous expression of the degradation pathway gene clusters, we selected 12 non-essential genes in the smaller chromosome of Vmax (chr. 2) as candidate targets for genome engineering through analysis of Vmax gene annotations (Supplementary Fig. 8) and whole-genome *V. natriegens* CRISPRi data[22] (Fig. 2g and Supplementary Table 4). To assess the feasibility of conducting gene knock-ins in these candidate target genes, reporter genes were integrated into each site using natural transformation to express sfGFP under the control of the constitutive P_{25} promoter. The *sfgfp* donor DNA was converted into three segments (an sfGFP gene and two 1-kb flanking sequences). The growth and fluorescence of each strain were analysed using a microplate reader. The result showed that VmaxΔchr2_182::*sfgfp* showed the lowest fluorescence intensity, and the other 11 variants ranged from 1.6×10^{-5} to 3.3×10^{-5} (Fig. 2h). We also found that chr2_297 yielded the highest (76.9%) integration efficiency, and inserting *sfgfp* at chr2_297 had no detrimental effects on the Vmax growth rate (Fig. 2i and Supplementary Fig. 9).

Insertion of degradation gene clusters

We selected nine previously characterized degradation gene clusters to produce strains capable of bioremediating organic pollutants. Each gene cluster was chemically synthesized and assembled in *Saccharomyces cerevisiae* before insertion into Vmax. The selected degradation gene clusters catabolized the monocyclic pollutants (benzene[23], toluene[24,25] and phenol[26]), dicyclic pollutants (naphthalene[27] and biphenyl[28]) and heterocyclic pollutants (DBF[29] and dibenzothiophene (DBT)[30]) (Supplementary Fig. 10 and Supplementary Table 5).

At present, the most often used size for synthetic DNA fragments in commercial applications is 3 kb, whereas fragments of approximately 5 kb are becoming increasingly affordable[31]. Therefore, we directly synthesized only gene clusters of less than 5 kb. The *bed*, *dmp*, *dbf* and *dsz* gene clusters were originally less than 5 kb. However, the *nah*, *bph* and *xyl* gene clusters exceeded 5 kb, were first synthesized in fragments of approximately 3 kb and then assembled into full-length gene clusters in vivo using *S. cerevisiae*. We noticed that some genes in the gene clusters overlapped with each other; therefore, we separated these genes. Ribosome binding sequences were included between the separated genes. All gene clusters were codon-optimized during synthesis (Supplementary Table 6). Nine candidate gene clusters with homology arms were ligated through restriction loci into the pRS415 shuttle plasmid and then amplified in *Escherichia coli*. The complete donor DNA fragment for each degradation gene cluster (containing the homology arm) was acquired from pRS415 through enzyme digestion or polymerase chain reaction (PCR) amplification (Supplementary Fig. 11).

Each gene cluster was separately integrated into the chr2_297 site of VCOD-2 and produced Vmax strains from VCOD-3 to VCOD-11 (Fig. 3a). Concentrated Vmax culturing was used for complex wastewater

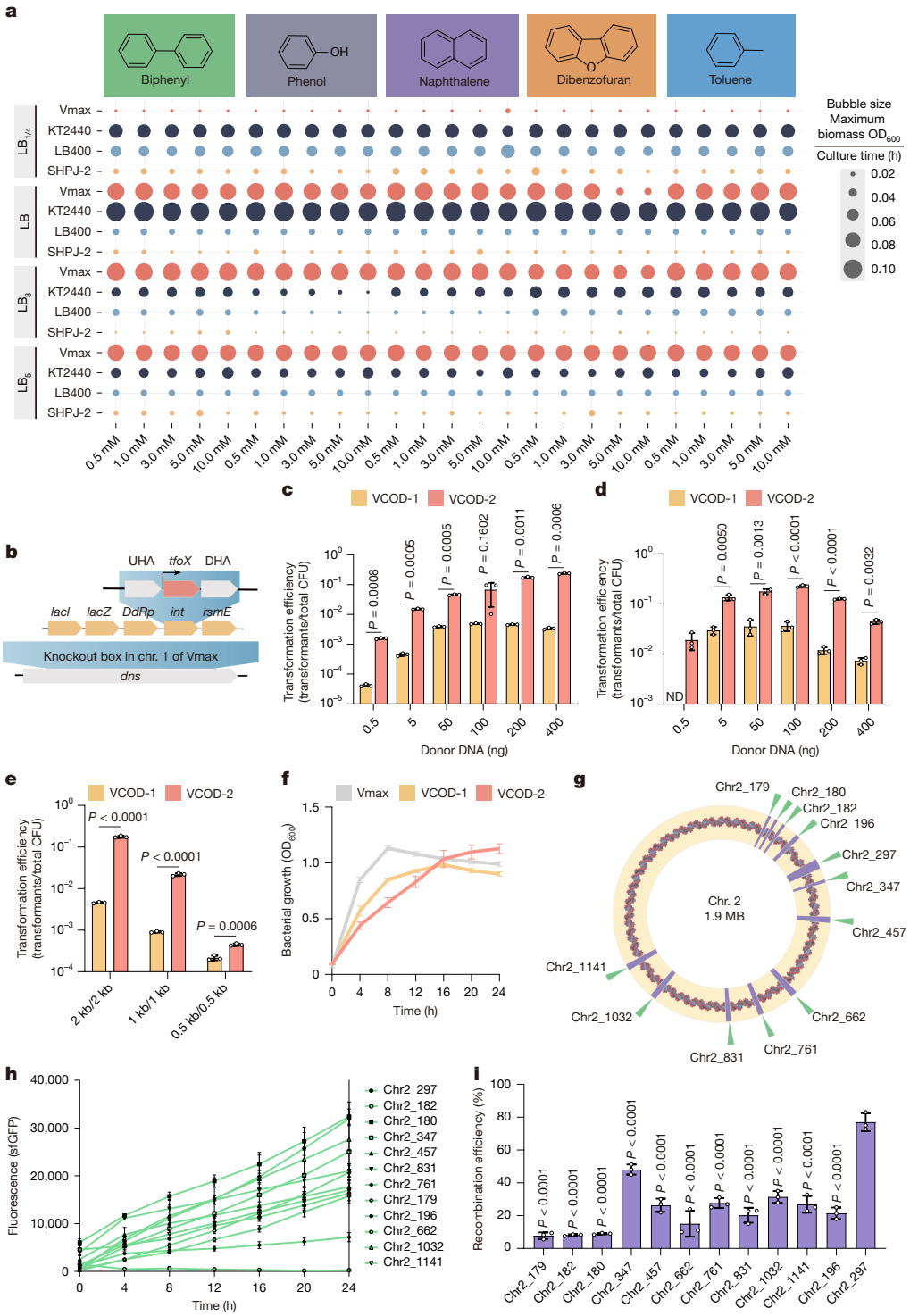

Fig. 2 | Development of a helper plasmid-free gene transfer method and selection of promoters for *V. natriegens*. **a**, Candidate strain growth rates in $LB_{1/4}$, LB, LB_3 and LB_5 media with pollutants (biphenyl, phenol, naphthalene, DBF and toluene, respectively). The bubble size represents the ratio of the maximum biomass (OD_{600}) to the culture time (h). The growth rate data in $LB_{1/4}$, LB, LB_3 and LB_5 media were derived from Supplementary Figs. 2–5. **b**, Schematic depicting the arrangement of *tfoX* insertion. The *lac* operator was inserted into the *int* site of *V. natriegens* ATCC 14048 to generate *V. natriegens* Vmax. The *tfoX* gene, regulated by the inducible promoter P_{T7}, was inserted at the *int* site in chr. 1 of Vmax, downstream of *DdRp* and upstream of *rsmE*. **c**, VCOD-2 transformation assay using 0.5–400 ng of p15A plasmid with natural transformation. **d**, VCOD-2 transformation assay using 0.5–400 ng of Δ*wbfF*::*Cm*^{R} (3 kb/3 kb) donor DNA in the chromosome with natural transformation. **e**, VCOD-2 transformation assay using 5 ng of Δ*wbfF*::*Cm*^{R} donor DNA containing the indicated homologous flanks with natural transformation. **f**, Growth of strains Vmax, VCOD-1 and VCOD-2 in LB_3 medium, measured as OD_{600}. **g**, Distribution of 12 neutral sites chosen as candidate insertion sites on chr. 2 of Vmax. **h**, Fluorescence of cells expressing sfGFP inserted at the 12 sites via natural transformation. **i**, The recombination efficiency of 12 sites was characterized using 2-kb flanking homologous fragments and *sfgfp* donor DNA. Statistical analysis: data are presented as mean ± s.d. of three independent experiments (**c**–**e**,**i**). Statistical significance was assessed using two-tailed unpaired *t*-test with Welch's correction (**c**–**e**) and Tukey's multiple comparison test (**i**). Data are presented as mean of three biological triplicates ± s.d. (**f**,**h**). *P* values are indicated above each genotype except VmaxΔchr2_297::*sfgfp* and relative to VmaxΔchr2_297::*sfgfp*. ND, not detected.

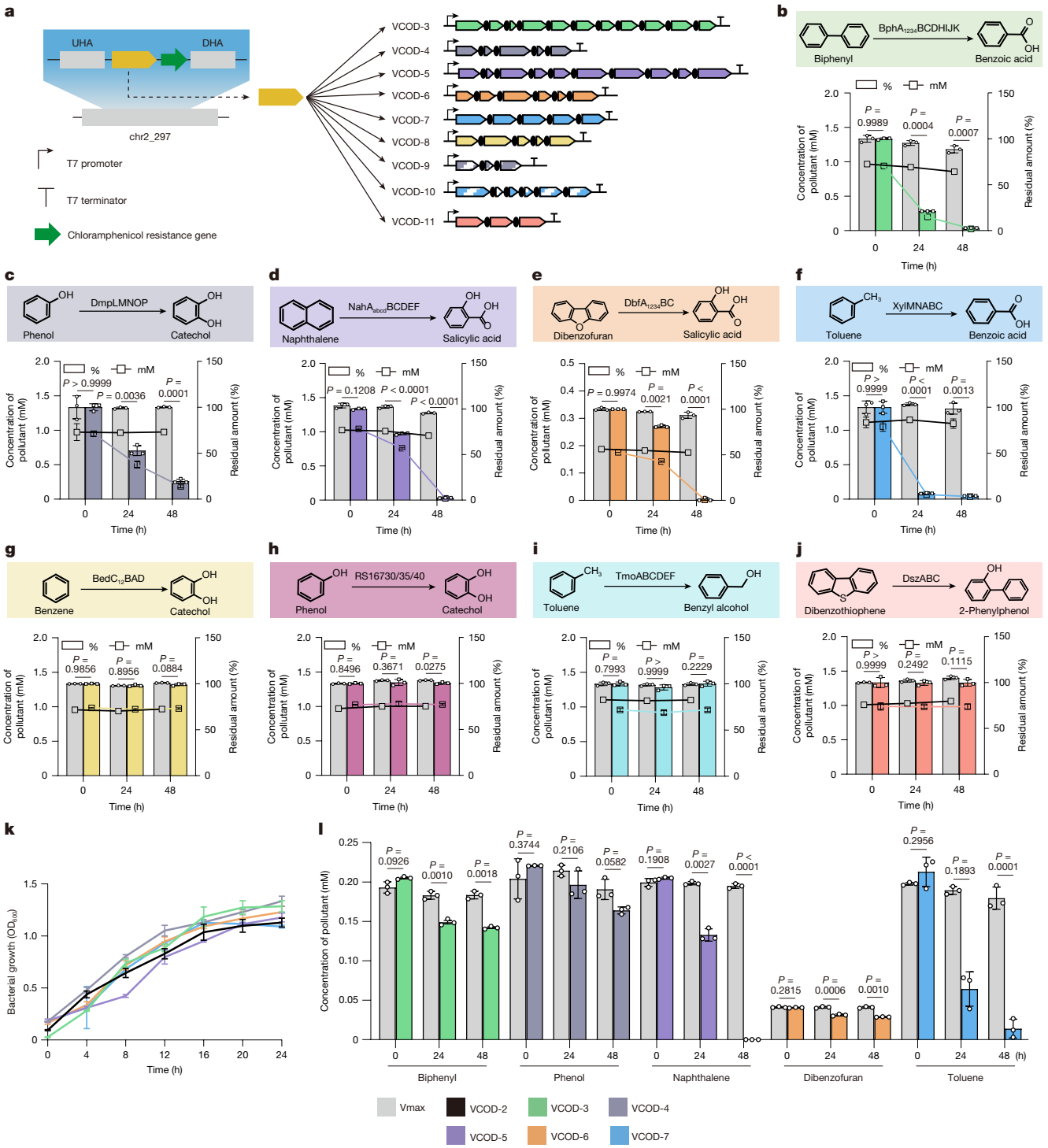

Fig. 3 | Insertion and in vivo examination of synthetic degradation gene clusters. a, Schematic illustration of gene cluster insertion with natural transformation. Nine synthetic degradation gene cluster fragments, each with 2-kb homologous arms on both sides, were inserted into the chr2_297 site of VCOD-2, and the engineered strains were sequentially numbered as VCOD-3 (Vmax Δ*int*::*tfoX* Δchr2_297::$bphA_{1234}BCKHJID$), VCOD-4 (Vmax Δ*int*::*tfoX* Δchr2_297::*dmpLMNOP*), VCOD-5 (Vmax Δ*int*::*tfoX* Δchr2_297::$nahA_{abcd}BFCYED$), VCOD-6 (Vmax Δ*int*::*tfoX* Δchr2_297::$dbfA_{1234}BC$), VCOD-7 (Vmax Δ*int*::*tfoX* Δchr2_297::*xylABCMN*), VCOD-8 (Vmax Δ*int*::*tfoX* Δchr2_297::$bedC_{12}BAD$), VCOD-9 (Vmax Δ*int*::*tfoX* Δchr2_297::*PPUTGB1_RS1673/16735/16740*), VCOD-10 (Vmax Δ*int*::*tfoX* Δchr2_297::*tmoABCDEF*) and VCOD-11 (Vmax Δ*int*::*tfoX* Δchr2_297::*dszABC*). **b**–**j**, Pollutant remediation efficiency of the engineered Vmax strains (**b**, VCOD-3; **c**, VCOD-4; **d**, VCOD-5; **e**, VCOD-6; **f**, VCOD-7; **g**, VCOD-8; **h**, VCOD-9; **i**, VCOD-10; **j**, VCOD-11). The coloured (engineered strain) and grey (Vmax, which served as the negative control) dots reflect the concentration of pollutants (left *y* axis). The coloured (engineered strain) and grey (Vmax) bars show the residual amounts of pollutants (right *y* axis). **k**, Growth of strains Vmax, VCOD-2 and engineered Vmax strains VCOD-2 to VCOD-7 in LB_3 medium, measured as OD_{600}. **l**, Complex organic pollutant remediation efficiency of the engineered consortium in NSS. The engineered consortium was generated by mixing the five engineered Vmax strains (VCOD-3 to VCOD-7). The complex organic pollutant mixture consisted of five organic compounds: biphenyl, phenol, naphthalene, DBF and toluene. Statistical analysis: data are presented as mean ± s.d. of three independent experiments (**b**–**j**,**l**). Statistical significance was assessed using unpaired *t*-test with Welch's correction. Data are presented as mean of three biological triplicates ± s.d. (**k**).

treatment in highly saline wastewater or offshore waters simulated using NSS. We observed a decrease in the concentration of biphenyl (from 938.6 to 26.2 μM), phenol (from 949.9 to 186.2 μM), naphthalene (from 1,043.2 to 26.3 μM), DBF (from 175.3 to 1.7 μM) and toluene (from 1,053.2 to 37.8 μM) following treatment with VCOD-3, VCOD-4, VCOD-5, VCOD-6 and VCOD-7, respectively (Fig. 3b–f). Analysis using ultra-performance liquid chromatography–mass spectrometry demonstrated that catechol (the degradation product of phenol), salicylic acid (the degradation product of biphenyl, naphthalene and DBF) and benzoic acid (the degradation product of toluene) were formed. Mass spectrometry detection also identified multiple expected intermediate metabolites, including 2,2′,3-trihydroxybiphenyl (derived from biphenyl degradation), naphthalene-1,2-diol (derived from naphthalene degradation), biphenyl-2,3-diol and 2-hydroxy-2,4-pentadienoate (derived from DBF degradation) and benzyl alcohol (derived from toluene degradation) (Extended Data Fig. 4). Four of the engineered strains, including VCOD-8, VCOD-9, VCOD-10 and VCOD-11, did not exhibit the capacity to reduce the corresponding pollutants (benzene, phenol, toluene and DBT, respectively) (Fig. 3g–j).

The inserted genes were expressed across all transformed strains under the control of P_{T7}, induced by IPTG in Vmax strains (from VCOD-3 to VCOD-7) (Extended Data Fig. 5). Insertion of degradation gene clusters slightly improved the tolerance of strains to phenol and DBF and did not cause detrimental effects on the Vmax growth rate (Fig. 3k and Supplementary Fig. 12). Therefore, VCOD-3, VCOD-4, VCOD-5, VCOD-6 and VCOD-7 were chosen as candidate strains for the bioremediation of complex organic pollutants.

A synthetic consortium was constructed using the engineered strains VCOD-3, VCOD-4, VCOD-5, VCOD-6 and VCOD-7 for the remediation of complex mixtures of pollutants. The synthetic consortium decreased 30.8% of biphenyl (from 205.0 to 141.9 μM), 22.6% of phenol (from 220.6 to 170.7 μM), 100.0% of naphthalene (from 204.8 to 0 μM), 29.2% of DBF (from 40.6 to 28.8 μM) and 93.4% of toluene (from 212.8 to 14.0 μM) in 48 h (Fig. 3l).

Complex organic pollutant bioremediation

We sought to create a single strain containing all five degradation gene clusters to simultaneously treat five organic pollutants. To accomplish this, we used yeast to combine the five gene clusters into a multigene cluster with a total length of 43 kb. However, a single natural transformation event cannot integrate this cluster into the VCOD-2 genome. Therefore, we established a multigene cluster composite strain through iterative insertion of degradation gene clusters into the VCOD-2 genome.

Using VCOD-3 as the initial strain, four degradation gene clusters (*dmp*, *nah*, *dbf* and *xyl*) were inserted from the 5′ to the 3′ ends of chr. 2. In the donor DNA used for insertions, each gene cluster was downstream of a 2,000-bp sequence corresponding to the homology arm of the previous gene cluster and upstream of a 2000-bp sequence corresponding to the chr2_297 homology arm to enable integration into the chromosome[32]. Each gene cluster also possessed a selectable marker. The complete series of degradation gene clusters was inserted into the Vmax genome using two selectable markers (kanamycin and chloramphenicol). As each gene cluster was introduced, the previously used marker was overwritten owing to homologous recombination with the incoming gene cluster (Supplementary Fig. 13). As a fundamental strategy, we applied it to construct complex pollutant remediation strains; this method was designated INTIMATE.

Following each round of editing, we examined the functions of the new strains VCOD-12, VCOD-13 and VCOD-14. Functional evaluations of the three intermediate strains showed that VCOD-12 removed 100.0% of biphenyl (from 186.1 to 0 μM) and 26.6% of phenol (from 185.1 to 135.9 μM) (Extended Data Fig. 6c,d). VCOD-13 removed 100.0% of biphenyl (from 183.5 to 0 μM), 46.5% of phenol (from 223.4 to 119.6 μM) and 70.7% of naphthalene (from 195.7 to 57.4 μM) (Extended Data Fig. 7c–e). VCOD-14 removed 100.0% of biphenyl (from 194.3 to 0 μM), 35.0% of phenol (from 180.1 to 117.1 μM), 60.2% of naphthalene (from 211.1 to 84.1 μM) and 78.0% of DBF (from 37.2 to 8.2 μM) within 48 h (Extended Data Fig. 8c–f). The growth rates of the intermediate strains did not decrease significantly after insertion of the degradation gene clusters (Extended Data Figs. 6e, 7f and 8g).

The final strain obtained was VCOD-15, which we anticipated could remediate a complex polluted environment (Fig. 4a). All degradation genes in each cluster were efficiently transcribed (Fig. 4b). The concentrations of biphenyl (from 189.3 to 0 μM), phenol (from 203.1 to 59.6 μM), naphthalene (from 185.8 to 52.5 μM), DBF (from 40.6 to 4.3 μM) and toluene (from 201.7 to 20.3 μM) exhibited a simultaneous decrease upon treatment with VCOD-15 (Fig. 4c–g). VCOD-15 successfully removed 100.0% of biphenyl, 60.7% of phenol, 71.8% of naphthalene, 89.3% of DBF and 89.9% of toluene in 48 h. We evaluated the growth ability of VCOD-15 and found no decrease relative to that of VCOD-2 (Fig. 4h). In addition, we detected anticipated metabolites of all five inserted gene clusters and did not identify new metabolites relative to the transformed single gene clusters (Extended Data Fig. 9). We examined the influence of the insertion of several gene clusters on the growth of the engineered strain and whether the gene clusters could stably exist in the genome. The genetic stability of VCOD-15 was assessed through continuous culture for 2 weeks. PCR amplification experiments have demonstrated the bridge regions across degradation gene clusters and their upstream/downstream sites (the bridge regions are also known as 'junctions') (Supplementary Table 7). Sanger sequencing findings also indicate that these junctions were consistent with the original sequence. From this, we inferred that they stably exist in the genome of VCOD-15 (Supplementary Fig. 14). These findings indicate that the constructed strain has genetic stability.

Pollutant remediation in wastewater

The multiple pollutant remediation capability of VCOD-15 was characterized. Five aromatic pollutants in NSS could be simultaneously remediated by VCOD-15; however, it is still unknown whether VCOD-15 maintains the same capability in saline and petroleum industrial wastewaters.

We collected industrial wastewater samples (named DL I and BZ I). The salinity in BZ I (102.5 g l^{-1}) was higher than in DL I (52.5 g l^{-1}), and Na^+ was the most abundant metal ion in the two industrial wastewater samples (34.8 and 16.2 g l^{-1}) (Supplementary Table 8). We examined the growth and pollutant tolerance ability of Vmax in the two wastewater samples and compared them with several other candidate chassis strains. Only Vmax could grow in BZ I, and Vmax maintained tolerance to organic pollutants in this industrial wastewater sample (Fig. 5a). In DL I, Vmax exhibited the highest final biomass (measured by OD_{600}) and fastest growth rate in the presence or absence of pollutants (Fig. 5b). These findings indicate that Vmax has advantages in adapting to industrial wastewater.

We compared the remediation ability of VCOD-15 with the natural degrading strains in BZ I and DL I. We chose biphenyl as the target pollutant and selected *P. putida* B6-2, the native host of the *bphA*$_{1234}$*BCKHJID* gene cluster, and LB400 as natural degrading strains[33]. In both wastewater samples, the residual amount of biphenyl-administered VCOD-15 was lower than B6-2 and LB400 (Fig. 5c,d).

We constructed an activated sludge reactor to implement bioremediation and verify the remediation process for the complex organic pollutants of VCOD-15 in industrial wastewater. A concentrated solution of the VCOD-15 culture was placed at the bottom of the container as the main component of the activated sludge. The wastewater to be remediated was then pumped into the container. Fresh air was pumped into the interface between the activated sludge

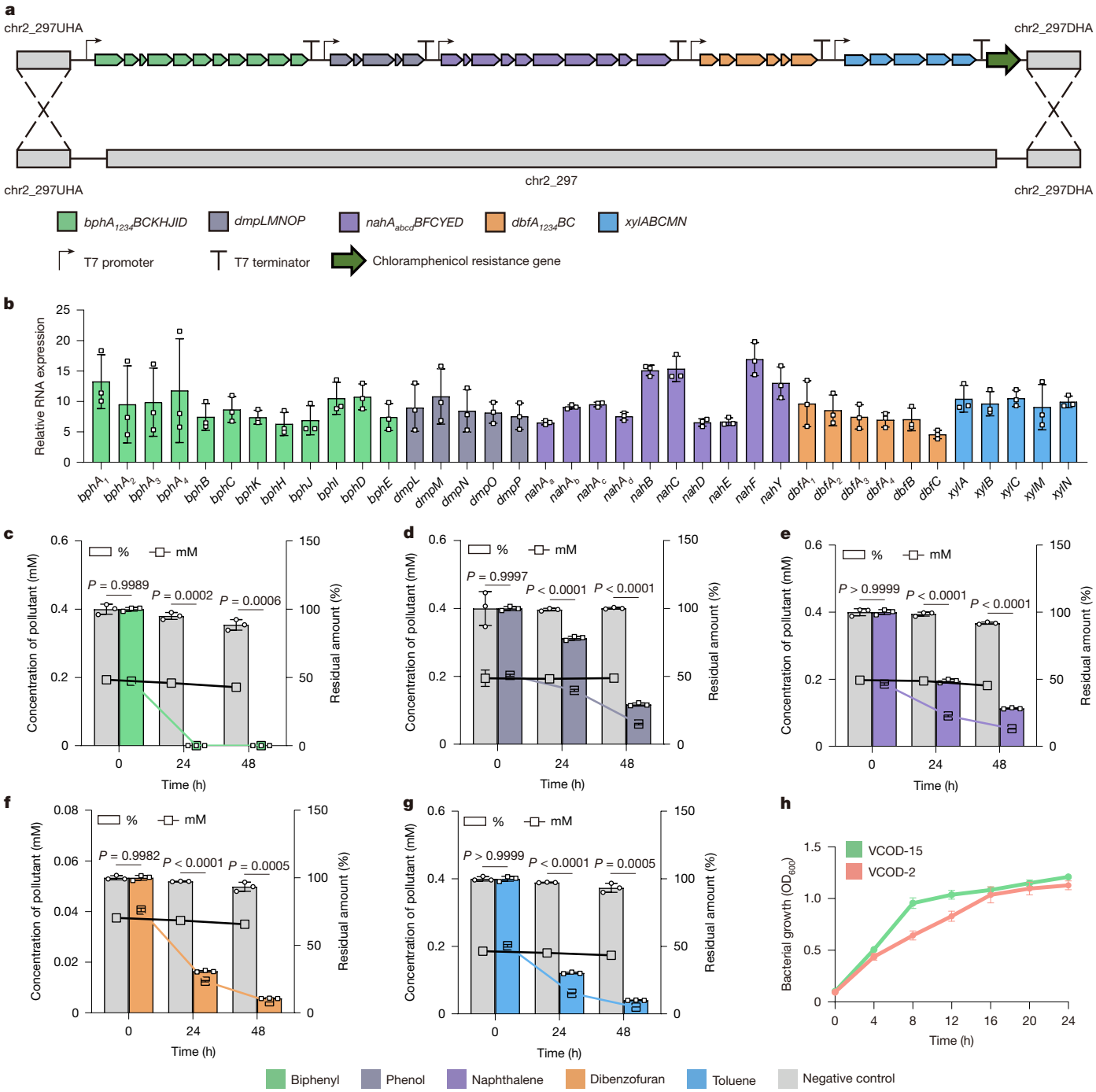

Fig. 4 | Examining the remediation of complex organic pollutants by VCOD-15 and gene expression levels. a, Schematic representation of the gene clusters inserted into the chromosome of VCOD-15 (Vmax*Δint*::*tfoX*Δchr2_297::*bphA*$_{1234}$*BCKHJID*::*dmpLMNOP*::*nahA*$_{abcd}$*BFCYED*::*dbfA*$_{1234}$*BC*::*xylABCMN*). Five gene clusters (*bph*, *dmp*, *nah*, *dbf* and *xyl*) were sequentially inserted into the neutral site chr2_297. The chloramphenicol resistance gene *Cm*^{R} is shown as a dark green arrow. The length of the concatenated gene clusters was 43 kb. **b**, Quantitative polymerase chain reaction (qPCR) analysis of the indicated genes from the complex pollutant-degrading gene cluster in engineered *V. natriegens* strain cultures, induced with 1 mM IPTG. **c**–**g**, Complex organic pollutant remediation efficiency of VCOD-15 in NSS. The mixture of complex organic pollutants consisted of five organic compounds (**c**, biphenyl; **d**, phenol; **e**, naphthalene; **f**, DBF; **g**, toluene). The coloured (VCOD-15) and grey (Vmax) dots reflect the concentration of pollutants (left *y* axis). The coloured (VCOD-15) and grey (Vmax) bars show the residual number of pollutants (right *y* axis). **h**, Growth of strains VCOD-2 and VCOD-15 in LB$_3$ medium was measured as OD$_{600}$. Statistical analysis: data are presented as mean of three biological triplicates ± s.d. (**b**). Data are presented as mean ± s.d. of three independent experiments (**c**–**g**). Statistical significance was assessed using unpaired *t*-test with Welch's correction. Data are presented as mean of three biological triplicates ± s.d. (**h**).

and wastewater using a ventilation pump, allowing sufficient oxygen for the reactions (Fig. 5e). VCOD-15 was cultured in LB$_3$ medium for 12 h and made into an activated sludge. After 12 h of reactions in the activated sludge bioreactor, all of the pollutants (1.0 mM biphenyl, 1.5 mM phenol, 1.1 mM naphthalene, 0.3 mM DBF and 1.2 mM toluene in BZ I; 1.2 mM biphenyl, 0.9 mM phenol, 1.0 mM naphthalene, 0.2 mM DBF and 1.3 mM toluene in DL I) were removed by VCOD-15 (Fig. 5f–j).

The capability of VCOD-15 was assessed in both flasks and activated sludge bioreactor with resting cells, thereby limiting its potential

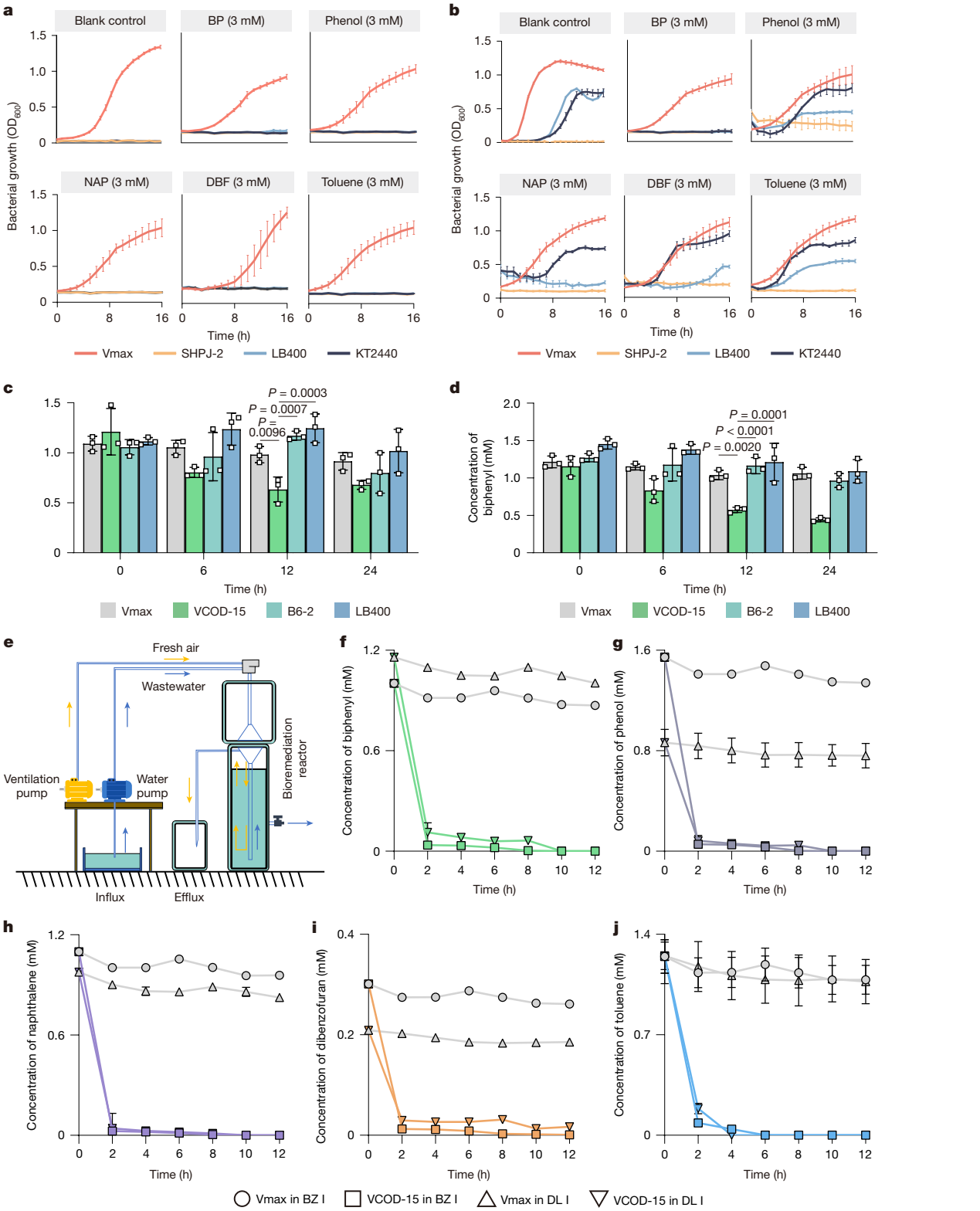

Fig. 5 | Bioremediation of complex polluted industrial wastewater samples in activated sludge bioreactor by VCOD-15. a,**b**, Growth of *V. natriegens* Vmax, *Sphingomonas* sp. SHPJ-2, *B. xenovorans* LB400 and *P. putida* KT2440 in industrial wastewater samples, measured as OD_{600}. Strains were cultured in wastewater samples BZ I (**a**) and DL I (**b**) added with 10 g l^{-1} yeast extract and the corresponding concentration of pollutants (shown in grey bar above the panel) at 30 °C with shaking. **c**,**d**, Biphenyl remediation efficiency of the strains Vmax, VCOD-15, *P. putida* B6-2 and *B. xenovorans* LB400 in industrial wastewater sample BZ I (**c**) and DL I (**d**). **e**, Schematic diagram of the activated sludge bioreactor, which was used for remediation of complex organic pollutants in industrial wastewater samples. **f**–**j**, Complex organic pollutant (**f**, biphenyl; **g**, phenol; **h**, naphthalene; **i**, dibenzofuran; **j**, toluene) remediation efficiency of VCOD-15 in industrial wastewater samples, performed in activated sludge bioreactor shown in **e**. Statistical analysis: data are presented as mean of three biological triplicates ± s.d. (**a**,**b**). Data are presented as mean ± s.d. of three independent experiments (**c**,**d**). Statistical significance was assessed using one-way analysis of variance (ANOVA) followed with Tukey's multiple comparison test. Data are presented as mean of three biological triplicates ± s.d. (**f**–**j**). Panel **e** was created using BioRender (https://biorender.com).

applications in remediating complex organic pollutants. We subsequently used VCOD-15 as a live bacterial agent for the remediation of complex organic pollutants in industrial wastewater samples using multi-parallel bioreactors (Extended Data Fig. 10a). We again collected industrial wastewater samples ('BZ II' and 'DL II'). We tested the growth of VCOD-15 using different carbon sources (yeast extract, corn steep liquor and molasses) in BZ II and DL II (Supplementary Fig. 15). We chose yeast extract as the carbon source. We added 1 g l^{-1} of yeast extract as the carbon source for BZ II and DL II. The organic pollutant concentrations and salinity were measured using high-performance liquid chromatography (HPLC) and/or gas chromatography and inductively coupled plasma–mass spectrometry (Supplementary Table 9). The industrial wastewater samples were added to the tanks of multi-parallel bioreactors without sterilization and mixed with the VCOD-15 culture. After 48 h of reaction in the bioreactors, the concentrations of five organic pollutants (biphenyl, phenol, naphthalene, DBF and toluene) remaining in BZ II were 15.3, 22.9, 13.2, 1.9 and 9.1 μM, respectively, whereas the concentrations in DL II were 22.0, 370.7, 33.5, 21.4 and 9.1 μM, respectively (Extended Data Fig. 10b–f). The results indicated that VCOD-15 removed 98.9% of biphenyl, 98.5% of phenol, 99.6% of naphthalene, 99.7% of DBF and 97.7% of toluene in BZ II, as well as 98.4% of biphenyl, 79.7% of phenol, 98.8% of naphthalene, 96.8% of DBF and 99.7% of toluene in DL II. To evaluate the viability of VCOD-15 in competition with the native strains in the industrial wastewater samples, we analysed the community composition at different times during wastewater treatment. The initial absence of *Vibrio* was observed in both samples before the introduction of VCOD-15. In BZ II, we observed relative abundances of 7.7%, 24.6% and 17.3% for *Vibrio* at 0, 24 and 48 h, respectively, during the remediation process. Similarly, in DL II, the relative abundances of *Vibrio* at these time points were 36.3%, 39.7% and 40.5%, respectively (Extended Data Fig. 10g).

Confirming pollutant degradation in soil

To assess the remediation potential of VCOD-15 in soil, we conducted bioremediation experiments using soil mixed with biphenyl (0.77 mmol kg^{-1}), phenol (1.06 mmol kg^{-1}), naphthalene (0.48 mmol kg^{-1}) and DBF (0.20 mmol kg^{-1}). Following an 8-day treatment with 10% (v/w) VCOD-15 bacterial suspension, VCOD-15 mediated net remediation of biphenyl (0.16 mmol kg^{-1}), phenol (0.66 mmol kg^{-1}), naphthalene (0.21 mmol kg^{-1}) and DBF (0.03 mmol kg^{-1}) (Supplementary Fig. 16). Soil samples were amended with both non-labelled and isotopically labelled pollutants: ^{13}C-labelled biphenyl and phenol, D-labelled naphthalene, DBF, biphenyl and phenol, followed by VCOD-15 treatment. High-resolution gas chromatography–mass spectrometry (HRGC–MS) analysis identified stable isotope-labelled intermediates within the metabolic pathways of all four pollutants during the flask-based remediation experiment (Supplementary Fig. 17). Consistent HRGC–MS profiles were subsequently observed in the soil remediation experiments (Supplementary Figs. 18–21).

Discussion

In this study, we engineered the *V. natriegens* strain VCOD-15 by iteratively integrating five degradation gene clusters (totalling 43 kb) into a neutral genomic site, enabling the remediation of complex organic pollutants in saline wastewater. However, VCOD-15 exhibits limitations. Its growth in low-salt environments is inferior to that of *P. putida* and *B. xenovorans*[34], and it cannot completely mineralize pollutants or use them as carbon sources unlike these bioremediation strains.

One major challenge is the inability of VCOD-15 to use pollutants as energy and carbon sources for growth. Introducing metabolic gene clusters for benzoic acid, catechol and salicylic acid could address this limitation, enabling complete pollutant mineralization. Moreover, we aim to adapt the gene cluster design and insertion strategies developed for VCOD-15 to other established degradation strains, such as *P. putida* KT2440, thereby expanding the applicability of engineered strains for diverse environments. Additionally, salinity tolerance genes from *V. natriegens*, such as *ectBACD* and *proWXV*, could be incorporated into *P. putida* KT2440 to enhance its performance under saline conditions[35]. Adaptive laboratory evolution offers another pathway to improve the robustness, tolerance, robustness and remediation efficiency of these strains[36].

Such engineered strains could be deployed to degrade complex organic pollutants in environments with fluctuating salinity, such as coastal marine areas polluted by freshwater effluents[37]. Furthermore, the substrate range of VCOD-15 can be expanded. Emerging marine pollutants, including azo dyes, organohalides and microplastics, pose significant challenges because of their resistance to degradation[38–40]. Recent studies have identified microbial strains capable of degrading these pollutants, such as the trypan blue-degrading strain *Vibrio* sp. JM-17[41], the organohalide-respiring strain *Desulfoluna spongiiphila* DBB[42] and the polyvinyl chloride-degrading strain *Klebsiella* sp. EMBL-1[43]. The degradation gene clusters from these strains could be integrated into VCOD strains to expand their capabilities.

To ensure environmental safety, biocontainment systems (such as suicide loops) could be incorporated into the genomes of engineered strains. Inducible promoters equipped with biosensors that are responsive to pollutants could enable controlled in situ degradation. Once remediation is complete, these microbial communities could safely exit the ecosystem[44].

V. natriegens offers significant advantages for genome engineering using tools such as natural transformation[45]. Using natural transformation, we developed the INTIMATE method, which enables iterative genome engineering. A current limitation of natural transformation is the requirement for long homology arms (approximately 2 kb) for optimal fragment integration (Fig. 2e). By contrast, the Red/ET recombination system requires only 30- to 50-bp homologous regions for efficient recombination[46]. By incorporating Red/ET recombination into VCOD-2 through natural transformation, we could develop a Red/ET-assisted INTIMATE system, enhancing the recombination efficiency. This would allow homology arms to be incorporated directly into the donor DNA during PCR amplification, streamlining the engineering process[47].

In summary, INTIMATE offers a robust platform for engineering next-generation strains with expanded substrate spectra, enhanced pollutant degradation capabilities and improved safety features. These strains could sense pollutants, self-destruct after remediation and integrate seamlessly into microbial communities to enhance environmental restoration efforts. Combining engineered strains with natural microbial communities could further increase bioremediation efficiency and address pressing environmental challenges.

Online content

Any methods, additional references, Nature Portfolio reporting summaries, source data, extended data, supplementary information, acknowledgements, peer review information; details of author contributions and competing interests; and statements of data and code availability are available at https://doi.org/10.1038/s41586-025-08947-7.

1. Duarte, C. M. et al. Rebuilding marine life. *Nature* **580**, 39–51 (2020).
2. Li, X. et al. High salinity inhibits soil bacterial community mediating nitrogen cycling. *Appl. Environ. Microbiol.* **87**, e01366–21 (2021).
3. Reddy, C. M. et al. Composition and fate of gas and oil released to the water column during the Deepwater Horizon oil spill. *Proc. Natl Acad. Sci. USA* **109**, 20229–20234 (2011).
4. Huynh, B. Q. et al. Public health impacts of an imminent Red Sea oil spill. *Nat. Sustainability* **4**, 1084–1091 (2021).
5. Dvořák, P. et al. Bioremediation 3.0: engineering pollutant-removing bacteria in the times of systemic biology. *Biotechnol. Adv.* **35**, 845–866 (2017).
6. Bhatt, P. et al. Biotechnological basis of microbial consortia for the removal of pesticides from the environment. *Crit. Rev. Biotechnol.* **41**, 317–338 (2021).

7. Atlas, R. M. & Hazen, T. C. Oil biodegradation and bioremediation: a tale of the two worst spills in U.S. history. *Environ. Sci. Technol.* **45**, 6709–6715 (2011).
8. Lin, J. et al. Environmental impacts and remediation of dye-containing wastewater. *Nat. Rev. Earth Environ.* **4**, 785–803 (2023).
9. Ahmadizadeh, R., Shokrollahzadeh, S., Latifi, S. M., Samimi, A. & Pendashteh, A. Application of halophilic microorganisms in osmotic membrane bioreactor (OMBR) for reduction of volume and organic load of produced water. *J. Water Process Eng.* **37**, 101422 (2020).
10. Weinstock, M. T. et al. *Vibrio natriegens* as a fast-growing host for molecular biology. *Nat. Methods* **13**, 849–851 (2016).
11. Eagon, R. G. *Pseudomonas natriegens*, a marine bacterium with a generation time of less than 10 minutes. *J. Bacteriol.* **83**, 736–737 (1962).
12. Ellis, G. A. et al. Exploiting the feedstock flexibility of the emergent synthetic biology chassis *Vibrio natriegens* for engineered natural product production. *Mar. Drugs* **17**, 679 (2019).
13. Teufel, M. et al. A multifunctional system for genome editing and large-scale interspecies gene transfer. *Nat. Commun.* **13**, 3430 (2022).
14. Stukenberg, D. et al. NT-CRISPR, combining natural transformation and CRISPR-Cas9 counterselection for markerless and scarless genome editing in *Vibrio natriegens*. *Commun. Biol.* **5**, 265 (2022).
15. Dalia, T. N. et al. Multiplex genome editing by natural transformation (MuGENT) for synthetic biology in *Vibrio natriegens*. *ACS Synth. Biol.* **6**, 1650–1655 (2017).
16. Lim, H. G. et al. *Vibrio* sp. dhg as a platform for the biorefinery of brown macroalgae. *Nat. Commun.* **10**, 2486 (2019).
17. Denkin, S. M. & Nelson, D. R. Induction of protease activity in *Vibrio anguillarum* by gastrointestinal mucus. *Appl. Environ. Microbiol.* **65**, 3555–3560 (1999).
18. Mutanda, I. et al. Bacterial membrane transporter systems for aromatic compounds: regulation, engineering, and biotechnological applications. *Biotechnol. Adv.* **59**, 107952 (2022).
19. Ramos, J. L. et al. Mechanisms of solvent tolerance in gram-negative bacteria. *Annu. Rev. Microbiol.* **56**, 743–768 (2002).
20. Hoff, J. et al. *Vibrio natriegens*: an ultrafast-growing marine bacterium as emerging synthetic biology chassis. *Environ. Microbiol.* **22**, 4394–4408 (2020).
21. Tschirhart, T. et al. Synthetic biology tools for the fast-growing marine bacterium *Vibrio natriegens*. *ACS Synth. Biol.* **8**, 2069–2079 (2019).
22. Lee, H. H. et al. Functional genomics of the rapidly replicating bacterium *Vibrio natriegens* by CRISPRi. *Nat. Microbiol.* **4**, 1105–1113 (2019).
23. Fong, K. P., Goh, C. B. & Tan, H. M. Characterization and expression of the plasmid-borne *bedD* gene from *Pseudomonas putida* ML2, which codes for a NAD+-dependent cis-benzene dihydrodiol dehydrogenase. *J. Bacteriol.* **178**, 5592–5601 (1996).
24. Assinder, S. J. & Williams, P. A. in Advances in Microbial Physiology, Vol. 31 (eds Rose, A. H. & Tempest, D. W.) 1–69 (Academic, 1990).
25. Kasai, Y., Inoue, J. & Harayama, S. The TOL plasmid pWW0 *xylN* gene product from *Pseudomonas putida* is involved in *m*-xylene uptake. *J. Bacteriol.* **183**, 6662–6666 (2001).
26. Liu, Y. et al. Phenol biodegradation by *Acinetobacter radioresistens* APH1 and its application in soil bioremediation. *Appl. Environ. Microbiol.* **104**, 427–437 (2020).
27. Simon, M. J. et al. Sequences of genes encoding naphthalene dioxygenase in *Pseudomonas putida* strains G7 and NCIB 9816-4. *Gene* **127**, 31–37 (1993).
28. Tang, H. et al. Genome sequence of *Pseudomonas putida* strain B6-2, a superdegrader of polycyclic aromatic hydrocarbons and dioxin-like compounds. *J. Bacteriol.* **193**, 6789–6790 (2011).
29. Kasuga, K. et al. Cloning of *dfdA* genes from *Terrabacter* sp. strain DBF63 encoding dibenzofuran 4,4a-dioxygenase and heterologous expression in *Streptomyces lividans*. *Appl. Microbiol. Biotechnol.* **97**, 4485–4498 (2013).
30. Denome, S. A., Olson, E. S. & Young, K. D. Identification and cloning of genes involved in specific desulfurization of dibenzothiophene by *Rhodococcus* sp. strain IGTS8. *Appl. Environ. Microbiol.* **59**, 2837–2843 (1993).
31. Jiang, S. et al. Efficient de novo assembly and modification of large DNA fragments. *Sci. China Life Sci.* **65**, 1445–1455 (2022).
32. Richardson, S. M. et al. Design of a synthetic yeast genome. *Science* **355**, 1040–1044 (2017).
33. Seeger, M. et al. Regiospecificity of dioxygenation of di- to pentachlorobiphenyls and their degradation to chlorobenzoates by the bph-encoded catabolic pathway of *Burkholderia* sp. strain LB400. *Appl. Environ. Microbiol.* **65**, 3614–3621 (1999).
34. de Lorenzo, V., Pérez-Pantoja, D. & Nikel, P. I. *Pseudomonas putida* KT2440: the long journey of a soil-dweller to become a synthetic biology chassis. *J. Bacteriol.* **206**, e00136-24 (2024).
35. Huang, L. et al. Establishment of a salt-induced bioremediation platform from marine *Vibrio natriegens*. *Commun. Biol.* **5**, 1352 (2022).
36. Sandberg, T. E. et al. The emergence of adaptive laboratory evolution as an efficient tool for biological discovery and industrial biotechnology. *Metab. Eng.* **56**, 1–16 (2019).
37. Yang, M. et al. Comparative toxicity of chlorinated saline and freshwater wastewater effluents to marine organisms. *Environ. Sci. Technol.* **49**, 14475–14483 (2015).
38. Lu, Q., Liang, Q. & Wang, S. Burning question: rethinking organohalide degradation strategy for bioremediation applications. *Microb. Biotechnol.* **17**, e14539 (2024).
39. Isobe, A. et al. Abundance of non-conservative microplastics in the upper ocean from 1957 to 2066. *Nat. Commun.* **10**, 417 (2019).
40. Si, J. et al. Porous composite architecture bestows Fe-based glassy alloy with high and ultra-durable degradation activity in decomposing azo dye. *J. Hazard. Mater.* **388**, 122043 (2020).
41. Khandare, S. D. et al. Biodegradation and decolorization of trypan blue azo dye by marine bacteria *Vibrio* sp. JM-17. *Biocatal. Agric. Biotechnol.* **51**, 102802 (2023).
42. Peng, P. et al. Organohalide-respiring *Desulfoluna* species isolated from marine environments. *ISME J.* **14**, 815–827 (2020).
43. Zhang, Z. et al. Polyvinyl chloride degradation by a bacterium isolated from the gut of insect larvae. *Nat. Commun.* **13**, 5360 (2022).
44. Liu, H. et al. An intelligent synthetic bacterium for chronological toxicant detection, biodegradation, and its subsequent suicide. *Adv. Sci.* **10**, 2304318 (2023).
45. Specht, D. A. et al. Efficient natural plasmid transformation of *Vibrio natriegens* enables zero-capital molecular biology. *PNAS Nexus* **3**, pgad444 (2024).
46. Lu, Q. Seamless cloning and gene fusion. *Trends Biotechnol.* **23**, 199–207 (2005).
47. Zheng, W. et al. Precise genome engineering in *Pseudomonas* using phage-encoded homologous recombination and the Cascade–Cas3 system. *Nat. Protoc.* **18**, 2642–2670 (2023).

Methods

Bacterial strains, media, chemicals and growth conditions

For plasmid propagation and cloning, the *E. coli* strains used were DH5α and Top10. All *E. coli* strains were grown in LB at 37 °C with shaking at 220 rpm. To produce a solid medium, 1.5% (w/v) agar was added to LB. The following antibiotics were added to the medium as required: 50 μg ml^{-1} kanamycin, 34 μg ml^{-1} chloramphenicol and 50 μg ml^{-1} ampicillin. All *V. natriegens* strains were grown in LB_3 at 30 °C or 37 °C with shaking at 220 rpm. Solid medium was prepared by adding 1.8% agar to the liquid medium. When needed, the following antibiotics were added to the medium: 200 μg ml^{-1} kanamycin, 9 μg ml^{-1} chloramphenicol and 10 μg ml^{-1} ampicillin. *P. putida* KT2440, *P. putida* B6-2 and *Sphingomonas* sp. SHPJ-2 were grown in LB medium at 30 °C with shaking at 220 rpm. *B. xenovorans* LB400 was grown in $LB_{1/4}$ at 30 °C with shaking at 220 rpm (ref. 48). Antibiotics were acquired from Inalco S.p.A. Phenol, toluene, naphthalene (NAP), biphenyl, DBF and DBT (purity of 99% or higher) were acquired from J&K Scientific. Biphenyl-$^{13}C_{12}$ was acquired from Toronto Research Chemicals (Chemical Abstracts Service number: 104130-36-1). Phenol-$^{13}C_1$, biphenyl-D_{10}, phenol-D_6, naphthalene-D_8 and dibenzofuran-D_8 were acquired from Sigma-Aldrich (Chemical Abstracts Service numbers: 70211-36-8, 1486-01-7, 13127-88-3, 1146-65-2 and 93952-04-6). All other chemical reagents were purchased from Merck-Sigma, unless otherwise indicated.

Growth curve measurement

Growth curves for the bacterial strains were measured using a Bioscreen C instrument. Strains were grown to log phase (OD_{600} of 0.4–0.5) by sub-culturing overnight bacterial culture 1:100 in LB medium at 30 °C and resuspended in corresponding media, and 5 μl of this normalized bacterial suspension was then inoculated into 100 μl of the desired growth media ($LB_{1/4}$, LB, LB_3, LB_5, LB_7, NSS and M9) in triplicates. Plates were incubated at 30 °C, and OD_{600} was measured every hour overnight while shaking continuously at high speed.

Transcriptomic analysis

VCOD-15 was cultured in LB_3 medium with high-concentration pollutants (4 mM biphenyl, 4 mM phenol, 4 mM naphthalene, 0.8 mM DBF and 4 mM toluene) or without the supplementation of complex organic pollutant mixture. The cells (6 h of cultivation) were collected by centrifugation (12,000 rpm; 4 °C; 15 min) and then frozen in liquid nitrogen. Total RNA was isolated using the TRIzol Reagent (Invitrogen Life Technologies). Quality and integrity were determined using a NanoDrop spectrophotometer (Thermo Fisher Scientific) and a Bioanalyzer 2100 system (Agilent). Zymo-Seq RiboFree Total RNA Library Kit was used to remove the ribosomal RNA from the total RNA. Random oligonucleotides and SuperScript III were used to synthesize the first-strand complementary DNA (cDNA). Second-strand cDNA synthesis was subsequently performed using DNA polymerase I and RNase H. The remaining overhangs were converted into blunt ends through exonuclease/polymerase activities, and the enzymes were removed. After adenylation of the 3′ ends of the DNA fragments, Illumina PE adaptor oligonucleotides were ligated to prepare them for hybridization. To select cDNA fragments of the preferred 400–500 bp in length, the library fragments were purified using the AMPure XP system (Beckman Coulter). DNA fragments with ligated adaptor molecules on both ends were selectively enriched using an Illumina PCR Primer Cocktail in a 15-cycle PCR reaction. The products were purified (AMPure XP system) and quantified using an Agilent high-sensitivity DNA assay on a 2100 Bioanalyzer system (Agilent). The sequencing library was then sequenced on a NovaSeq 6000 platform (Illumina) by Shanghai Personalbio. Raw sequence data were collected and filtered using Genescloud (Shanghai Personalbio). From the two constructed libraries of the three treatment groups (negative control and pollutant-induced), 2,602,294,177, 2,583,798,437 and 2,807,929,296 clean reads and 87,272,844, 84,163,224 and 81,043,456 clean reads were obtained, respectively. The reference genome and gene annotation files of *V. natriegens* were downloaded from the National Center for Biotechnology Information (NCBI). The reference genome index was built using Bowtie 2 (v.2.5.1), and the filtered reads were mapped to the reference genome using Bowtie 2 (http://bowtie-bio.sourceforge.net/index.shtml). The gene read count value was counted using HTSeq (v.0.9.1) as the original expression level of the gene. To make the gene expression levels of different genes and different samples comparable, fragments per kilobase of exon per million mapped fragments was used to normalize the expression. Differentially expressed messenger RNA was analysed using DESeq (v.1.30.0). Transcripts with $|\log_2\text{-fold change}|$ greater than 1 and P value less than 0.05 were considered differentially expressed. The heat map was plotted using Bioinformatics (https://www.bioinformatics.com.cn; last accessed on 30 August 2024), an online data analysis and visualization platform.

QPCR for assessing the transcription of genes

To remove potential DNA contamination, total RNA was treated with 1 U DNase I (EN0521; Thermo Fisher Scientific) for 20 min at 37 °C and purified using a Bacterial Total RNA Extraction Kit (catalogue no. DP430; TIANGEN). Total RNA (1.0–3.0 μg) was reverse transcribed to cDNA using the SuperScript III First-Strand Synthesis System (18080051; Invitrogen). The same amount of total RNA was used for direct comparison. QPCR was conducted using iQ SYBR Green Supermix (1708880; Bio-Rad) with 150 nM primers in a 10-μl reaction. Amplifications were performed with the following protocol for all experiments: 95 °C for 10 min, followed by 40 cycles of 95 °C for 15 s, 58 °C for 15 s and 68 °C for 20 s. The specificity of primer pairs was examined using melting curves at the end of the 40th amplification cycle. The *rpoD* gene encoding a sigma factor for transcription initiation was selected as an internal housekeeping gene and was used as the baseline control for evaluating the expression of the degradation genes[49]. Relative RNA expression represents the relative expression level. See Supplementary Table 10 for the primers used in qPCR.

Generation of reporter strains and time-lapse analysis

The reporter strains for mutagenesis were derived from Vmax. The fragments flanked by arms complementary to the promoter scaffold were amplified by means of PCR using Phusion PCR Master Mix (New England Biolabs) and cloned into the p15A and pET28a vectors via Gibson Assembly according to the manufacturer's protocol. The OD_{600} values and fluorescence signals were examined, and glycerol stocks of bacteria stored at −80 °C were streaked on non-resistant or agar plates containing the corresponding antibiotics to isolate single colonies. A single colony was inoculated into a test tube containing 3 ml of LB_3 (supplemented with the appropriate antibiotic corresponding to the strain resistance gene) and cultured in a shaker at 30 °C with shaking at 220 rpm. After approximately 12 h of growth, the bacterial solution was added to fresh LB_3 at OD_{600} of 0.1. Culturing was continued in a shaker at 30 °C with shaking at 220 rpm until the culture in each test tube reached the mid-log phase. Each culture was diluted to OD_{600} of 0.07–0.09 and inoculated into a 96-well plate (Costar; black; clear bottom), adding 150 μl per well. LB_3 wells with antibiotics were used for resistant strains, and LB_3 wells lacking antibiotics were used for the Vmax and VCOD-2 strains. Each 96-well plate contained at least three wells without inoculation, and only LB_3 was added as a negative control. A microplate reader (Infinite M Plex 200 PRO) was used to obtain the OD_{600} and fluorescence absorption data in a black 96-well microtitre plate, and the parameters were established using Tecan i-control software. The fluorescence intensity was assessed as follows: the sfGFP excitation wavelength was established at 480 nm, and the detection wavelength was established at 510 nm. The fluorescence intensity scan mode was executed as follows: for sfGFP excitation,

the wavelength was 475 nm, and the emission wavelength detection range was 495–750 nm. The black 96-well plate was cultured by undergoing continuous shaking on the plate microplate reader, and the OD_{600} and fluorescence measurements were recorded every 20 min. All experiments were conducted using three technical replicates (three replicate wells) and two to three independent experiments. The fluorometry data were processed using Tecan i-control software and exported to Microsoft Excel 2019 and GraphPad Prism v.8.3.1 for data analysis.

Preparation of electrocompetent cells and electroporation of *V. natriegens*

An overnight culture of *V. natriegens* was pelleted, rinsed once with fresh medium and diluted 1:100 in growth medium. The culture was grown at 37 °C in a flask with shaking at 220 rpm until reaching OD_{600} of 0.5. The culture was transferred to a 50-ml centrifuge tube and centrifuged at 6,500 rpm in a himacR18A-4020 centrifuge rotor for 15 min at 4 °C. The supernatant was carefully removed, and the cell pellets were carefully resuspended in 30 ml of electroporation buffer (680 mM sucrose and 7 mM K_2HPO_4 (pH 7.0) and inverted several times to combine. The cells were centrifuged at 6,750 rpm for 15 min at 4 °C in the himacR18A-4020 rotor. The supernatant was removed, and the wash was repeated twice for a total of three washes. Following the final wash, the cell pellet was carefully resuspended in residual electroporation buffer (resulting in a final OD_{600} of 16.0). For long-term storage, competent cells were aliquoted into 50-µl aliquots in pre-chilled tubes, frozen using liquid nitrogen and stored at −80 °C for future use. Plasmid DNA (1.0 µg) was added to 100 µl of electrocompetent cells and gently mixed in a chilled 1.5-ml microcentrifuge tube without producing air bubbles. The cell–DNA suspension was transferred to a chilled electroporation cuvette with a 1-mm gap size and electroporated using a Bio-Rad Gene Pulser electroporator at 0.9 kV, 1 kΩ and 25 µF. To avoid unnecessary cell death, the electroporated cells were immediately recovered in 0.5 ml of recovery medium (LB_3 or SOC medium containing 680 mM sucrose, lacking any antibiotics) and transferred to a 1.5-ml microcentrifuge tube. The cells were then recovered after incubation at 37 °C for 1 h. Aliquots of the recovery medium were plated on warm selective agar plates containing the appropriate antibiotics. The plates were incubated for 8 h at 37 °C or 12 h at 30 °C to allow colonies to appear.

Natural transformation of VCOD-1

V. natriegens strains containing pET28a-*tfoX* were induced by growing overnight (15 h) in LB_3 supplemented with 200 µg ml^{-1} kanamycin and 0.1 mM IPTG in an orbital shaker incubator at 30 °C. Then, 3.5 µl of the culture was diluted directly into 350 µl of Instant Ocean medium (IOM; 28 g l^{-1}) supplemented with 0.1 mM IPTG. Approximately 300 ng of transforming DNA was added as indicated, and the reactions were incubated statically at 30 °C for 6 h. Next, 1 ml of LB_3 was added, and the reactions underwent outgrowth at 30 °C with shaking (220 rpm) for 2 h. The culture was spread on a bi-antibiotic LB_3 agar plate (containing 200 µg ml^{-1} kanamycin and 9 µg ml^{-1} chloramphenicol) to select for integration of the selected product.

Natural transformation optimization with VCOD-2

VCOD-2 was induced by growing overnight (final OD_{600} of 3.8–4.2) in LB_3 supplemented with 0.1 mM IPTG in the orbital shaker incubator at 30 °C. Then, 3.5 µl of the culture was diluted directly into 350 µl of IOM (28 g l^{-1}) supplemented with 0.1 mM IPTG. Approximately 200 ng of transforming donor DNA (homologous arms of 2 kb) or 100 ng of plasmid was added as indicated, and the reaction was incubated statically at 30 °C for 6 h. Next, 1 ml of LB_3 was added, and the reactions underwent outgrowth at 30 °C with shaking (220 rpm) for 2 h. The culture was then spread on a bi-antibiotic LB_3 agar plate to select for integration of the selected product.

Designing of the synthetic degradation gene clusters

The synthetic degradation gene clusters were designed using the following pipeline[50]. Known natural degradation and metabolism gene cluster sequences were identified (step 1). The gene cluster was annotated by (1) listing all degradation metabolism-related functions encoded in the gene cluster and (2) finding the corresponding coding DNA sequence (CDS) for each known function (step 2). The presence of each function in the synthetic gene cluster was verified by ensuring that (1) each degradation-related function had a unique CDS corresponding to it and (2) each CDS corresponded to a unique degradation function (step 3). All CDSs were codon-optimized according to the codon preference of *V. natriegens* (Supplementary Table 6), so that the translated protein sequence remained unchanged, although the codon was one of the degenerate codons with the highest frequency of corresponding amino acids in *V. natriegens* (step 4). The ribosome binding sequence (B0029, B0030, B0034, and B0035; Supplementary Table 3) was added before all CDSs (step 5). The CDSs were arranged from 5′ to 3′ on the original gene cluster to obtain the gene sequence (step 6). A P_{T7} promoter was added at the 5′ end of the gene cluster sequence, and a T7 terminator was added at the 3′ end of the gene cluster sequence (step 7). The designed gene cluster sequence of the synthetic gene cluster was finalized (step 8).

Preparation of resting cells and degradation test

The strains were activated in LB_3 for 1 h, collected following growth to the late logarithmic phase (approximately 10 h after IPTG induction), rinsed three times and resuspended in NSS. The final optical density at 600 nm was adjusted to 8.0–10.0. The cells were then starved at 30 °C for 2 h. After culturing at 30 °C with shaking at 200 rpm for 0, 6, 12, 24, 36 and 48 h, an equal volume of ethyl acetate was added to the cultures, followed by vortexing (45 W for 2 min) and centrifugation (8,000 rpm for 5 min). The liquid phase was collected for HPLC detection. The initial concentrations of organic pollutants were established as follows: 1 mM biphenyl, 1 mM phenol, 1 mM NAP, 0.2 mM DBF and 1 mM toluene. To examine the degradation of VCOD-15 and other engineered strains containing more than one degradation gene cluster, the initial concentrations of organic pollutants were set as follows: 0.2 mM phenol, 0.2 mM toluene, 0.2 mM NAP, 0.2 mM biphenyl and 0.04 mM DBF.

Industrial wastewater sample collection and characterization

DL I and DL II were collected from a petroleum refinery at Sinopec Chemical Industrial. BZ I and BZ II were collected from BEFAR GROUP. The salinity and concentration of primary metal salt ions in the industrial wastewater samples were measured using a conductivity meter and inductively coupled plasma–mass spectrometry.

Organic pollutant mixture remediation in activated sludge bioreactor

VCOD-15 was cultured in LB_3 for 1 h, collected following growth to the late logarithmic phase (approximately 10 h after IPTG induction), rinsed three times, resuspended in saline industrial wastewater sample and concentrated into a solution with OD_{600} of 12.0. The solution was placed at the bottom of the reactor as the main decomposer of the activated sludge. Then, 1 l of the wastewater sample was immediately added to the reactor. The entire reaction was conducted with a ventilation flow rate of 200 l h^{-1} at room temperature (approximately 25 °C). After remediation for 0, 2, 4, 6, 8 and 12 h, 10 ml of wastewater was sampled, and then an equal volume of ethyl acetate was added to the cultures, followed by vortexing and centrifugation. The liquid phase was collected for HPLC detection.

Organic pollutant mixture remediation in multi-parallel bioreactors

A total of 0.5-g yeast extract, 153.1-mg biphenyl, 94.1-mg phenol, 128.17-mg naphthalene, 33.7-mg DBF and 87.2-mg toluene were added

to 0.5 l of the wastewater sample and sufficiently stirred in the tank of multi-parallel bioreactors to ensure even distribution of pollutants in the wastewater sample. The salinity was measured using a conductivity meter. Major ion and organic pollutant concentrations were measured using ICP, HPLC equipped with diode array detector (DAD) and/or gas chromatography equipped with flame ionization detector (FID) (Supplementary Table 9). The wastewater sample was not sterilized, and the remediation test was conducted in an open system. VCOD-15 was cultured in LB_3 medium. The cell solution (50 ml) was added to 450 ml of the wastewater sample. IPTG (0.1 mM) was added to the wastewater/VCOD-15 sample to induce the expression of the degradation gene clusters. The temperature of the wastewater sample in the tank was maintained at 30 °C with stirring at 200 rpm, and air was supplied at a speed of 200 l h^{-1}. Then, 2 ml of the water sample was collected every 12 h for 48 h, mixed with 2-ml ethyl acetate and vortexed. The extracted residual pollutants were measured using an Agilent Technologies HPLC 1200/1260 series equipped with DAD and an Agilent Technologies 8890 GC System equipped with FID.

Analytical methods

Each aromatic contaminant was identified and quantified using HPLC (Agilent Technologies 1200/1260 series) using a variable-wavelength detector and an Agilent Eclipse XDB-C18 column (4.6 × 150 nm; 5 µm). The mobile phase flow rate was 0.8 ml min^{-1} and was held for 15 min. Phase A consisted of Q1 H_2O (added with 0.1% methane acid; v/v), and phase B consisted of acetonitrile. The detection wavelengths were 254 nm (naphthalene and biphenyl), 275 nm (phenol) and 280 nm (DBF and DBT).

Toluene and benzene were detected and quantified using the Agilent Technologies 8890 GC System equipped with an Agilent 7697 headspace autosampler, a DB-1301 column and an FID detector. The Agilent 8890 GC oven was maintained at 60 °C for 1 min, followed by an increase of 5 °C min^{-1} to 165 °C and then 25 °C min^{-1} to a final temperature of 300 °C, which was held for 14 min. The volume of the injected sample was 10 µl.

The intermediate metabolites of various substrates were prepared using a previously described method[51]. The extraction was detected and analysed using ultra-performance liquid chromatography coupled with quadrupole time-of-flight mass spectrometry (UPLC–QTOF-MS) (Agilent 1290 Infinity LC with 6230 quadrupole mass spectrometry). The HPLC and UPLC–QTOF-MS for PAHs and heterocyclic derivatives were performed using an Agilent Eclipse XDB-C18 column (4.6 × 150 nm; 5 µm) using the previously described method, in which the flow rate was modified to 0.8 ml min^{-1}, and 0.1% (v/v) formic acid was added to deionized water[52]. Mass spectrometry was conducted in electrospray ionization negative-ion mode.

Microbial diversity analysis in industrial wastewater samples

Total genomic DNA samples were extracted using the PureLink Genomic DNA Purification Mini Kit (Invitrogen), following the manufacturer's instructions, and stored at −20 °C before further analysis. The quantity and quality of the extracted DNA samples were measured using a NanoDrop NC2000 spectrophotometer (Thermo Fisher Scientific) and agarose gel electrophoresis, respectively. PCR amplification of the bacterial 16S ribosomal RNA gene V3–V4 region was performed using the forward primer 338F (5′-ACTCCTACGGGAGGCAGCA-3′) and reverse primer 806R (5′-GGACTACHVGGGTWTCTAAT-3′). Sample-specific 7-bp barcodes were incorporated into the primers for multiplex sequencing. The PCR components contained 5 µl of buffer (5×), 0.25 µl of FastPfu DNA Polymerase (5 U $µl^{-1}$), 2 µl (2.5 mM) of deoxynucleotide triphosphates, 1 µl (10 µM) of each forward and reverse primer, 1 µl of DNA template and 14.75 µl of ddH_2O. Thermal cycling consisted of initial denaturation at 98 °C for 5 min, followed by 25 cycles of denaturation at 98 °C for 30 s, annealing at 53 °C for 30 s and extension at 72 °C for 45 s, with a final extension of 5 min at 72 °C. PCR amplicons were purified using Vazyme VAHTS DNA Clean Beads and quantified using the Quant-iT PicoGreen dsDNA Assay Kit (Invitrogen). After the individual quantification step, amplicons were pooled in equal amounts, and pair-end 2 × 250 bp sequencing was performed using an Illumina NovaSeq platform with a NovaSeq 6000 SP Reagent Kit (500 cycles) from Shanghai Personalbio.

Bioinformatics was performed with QIIME 2 2022.11 with slight modifications according to the official tutorials (https://docs.qiime2.org/2022.11/tutorials/). Briefly, raw sequence data were demultiplexed using the demux plugin, followed by primer cutting using the cutadapt plugin. Sequences were then quality-filtered, denoised, merged and chimeras removed using the DADA2 plugin. Non-singleton amplicon sequence variants were aligned with MAFFT and used to construct a phylogeny using FastTree 2. Taxonomy was assigned to amplicon sequence variants using the classify-sklearn naive Bayes taxonomy classifier in a feature-classifier plugin against the SILVA Release 138.1 database. Principal component analysis was also conducted on the basis of genus-level compositional profiles. The significance of differentiation of microbiota structure among groups was assessed by permutational multivariate analysis of variance, analysis of similarities and permdisp using QIIME 2. The taxonomic compositions and abundances were visualized using MEGAN, GraPhlAn and ChiPlot (https://www.chiplot.online/).

Soil remediation by VCOD-15

To prepare a complex organic polluted saline soil sample, bulk Danish peat soil (Pindstrup Mosebrug A/S) was doused with an aqueous 30 g kg^{-1} NaCl solution and sufficiently shaken. Complex organic pollutant liquor (60 ml) was sprayed into a 3-kg saline soil sample, and then the soil was sufficiently mixed. A 25-g sample of the soil sample was mixed with 25-ml ethyl acetate and then vortexed. After extraction with an equal volume of ethyl acetate, the mixture was centrifuged at 8,000 rpm for 10 min to separate the supernatant organic layer. The concentration of pollutants in the sample was measured using the Agilent Technologies HPLC 1200/1260 series equipped with DAD. The remaining soil was acidified to pH 2.0 using 6 M HCl and subjected to secondary ethyl acetate extraction. The resultant organic phase from both extractions was combined, evaporated to dryness under a N_2 stream using a TurboVap concentrator and reconstituted to 1/100th of the original volume. The concentrated extract was derivatized with bis(trimethylsilyl)trifluoroacetamide at 70 °C for 0.5 h to enhance volatility, followed by analysis using gas chromatography coupled with HRGC–MS (Orbitrap Exploris GC 240; Thermo Fisher Scientific) in chemical ionization mode.

Calculation of net biodegradation capacity of VCOD-15

The net biodegradation capacity of VCOD-15 was calculated by subtracting abiotic losses (adsorption/volatilization) observed in the phosphate-buffered saline-treated control group from the total removal in the VCOD-15-treated group. For each pollutant, background-corrected degradation was determined as follows:

Net degradation concentration (mmol kg^{-1}) = (initial concentration$_{VCOD\text{-}15}$ − final concentration$_{VCOD\text{-}15}$) − max((initial concentration$_{negativecontrol}$ − final concentration$_{negativecontrol}$), 0)

Negative values in control groups (indicating no net abiotic loss) were set to 0 to avoid overestimating biological contributions[53].

Statistical analysis

Primary data processing and organization were performed in Microsoft Excel (2021). Statistical analyses were performed using GraphPad Prism v.8. Statistical significance between two groups was determined using an unpaired two-tailed *t*-test. In the case of unequal variance between the two groups, the unpaired Welch's *t*-test was used. To determine the differences between more than two groups, one-way ANOVA was applied. Depending on the scientific question, one-way ANOVA was

followed by no post hoc test or Tukey's post hoc test (comparing all groups), as indicated in the figure legends. Data are expressed as the mean, and the error bars indicate the s.d. unless otherwise specified[54]. A detailed description of the statistics is provided in the figure legends. Statistical significance was defined as $^{*}P < 0.05$, $^{**}P < 0.01$, $^{***}P < 0.001$ and $^{****}P < 0.0001$. NS denotes not significant.

Reporting summary

Further information on research design is available in the Nature Portfolio Reporting Summary linked to this article.

Data availability

The genome assembly generated in this study was deposited in NCBI under the BioProject PRJNA1240198. All other data are presented in the paper and Supplementary Information. The public data used in this study included function annotations of non-essential genes in the genome of Vmax and degradation gene clusters from the NCBI database (https://www.ncbi.nlm.nih.gov). The accession numbers of the genes are listed in Supplementary Tables 4 and 5.

48. Bopp, L. H., Chakrabarty, A. M. & Ehrlich, H. L. Chromate resistance plasmid in *Pseudomonas fluorescens*. *J. Bacteriol.* **155**, 1105–1109 (1983).
49. Gal-Mor, O. et al. A novel secretion pathway of *Salmonella enterica* acts as an antivirulence modulator during salmonellosis. *PLoS Pathog.* **4**, e1000036 (2008).
50. Chan, L. Y., Kosuri, S. & Endy, D. Refactoring bacteriophage T7. *Mol. Syst. Biol.* **1**, 2005.0018 (2005).
51. Gai, Z. et al. Cometabolic degradation of dibenzofuran and dibenzothiophene by a newly isolated carbazole-degrading *Sphingomonas* sp. strain. *Appl. Environ. Microbiol.* **73**, 2832–2838 (2007).
52. Liu, Y. et al. A *Pseudomonas* sp. strain uniquely degrades PAHs and heterocyclic derivatives via lateral dioxygenation pathways. *J. Hazard. Mater.* **403**, 123956 (2021).
53. Gressel, S. et al. CDK9-dependent RNA polymerase II pausing controls transcription initiation. *eLife* **6**, e29736 (2017).
54. Biglari, N. et al. Functionally distinct POMC-expressing neuron subpopulations in hypothalamus revealed by intersectional targeting. *Nat. Neurosci.* **24**, 913–929 (2021).

Acknowledgements This study was supported by the National Key Research and Development Program of China (2021YFA0909500), National Natural Science Foundation of China (32030004, 32150025 and 82003626), Guangdong S&T Program (2022B1111080005, 2022A0505090009), Shenzhen Science and Technology Program (KQTD20180413181837372), Innovation Program of Chinese Academy of Agricultural Science and the Shenzhen Outstanding Talents Training Fund. We would like to thank the Core Facility and Service Center for School of Life Sciences and Biotechnology, SJTU for the metabolite analysis data collection. We would also like to thank Y. Li from Shanghai Jiao Tong University for his insightful and valuable assistance in the metabolism testing of stable isotope-labelled compounds and in the analysis of the GC–HRMS data, as well as Q. Wang from Tianjin Institute of Industrial Biotechnology, Chinese Academy of Sciences for his kind provision of the experimental material IOM.

Author contributions H.T. and J.D. designed and supervised the overall research framework and provided acquired funding. C.S., Y. Liu, C.W. and L.Q. conducted molecular biology experiments, including bacterial strain construction, transcriptomic analyses and qPCR gene expression analysis. C.S., H.C. and P.Z. performed bacterial growth characterization and pollutant degradation assays, including optimization of culture conditions, growth curve measurement and degradation testing. H.C., W.W., Z.C., M.Y., Y. Li and S.H. collected and processed industrial wastewater and soil samples and conducted pollutant degradation experiments under practical environmental conditions. C.S., H.C., W.W., Z.C., M.Y., Y. Li, P.X. and H.T. performed chromatographic and mass spectrometric analyses (HPLC, gas chromatography, UPLC–QTOF-MS and HRGC–MS) and conducted data analysis. H.C., W.W., Z.C., M.Y. and Y. Li conducted microbial diversity analyses of environmental samples and performed statistical analyses, data organization and significance testing. C.S., H.C., W.W., Z.C., M.Y., Y. Li, Y.C., S.H., J.Z., P.X., J.D. and H.T. wrote the paper. All authors contributed to reviewing the draft of the paper and approving the final paper.

Competing interests The authors declare no competing interests.

Additional information

Supplementary information The online version contains supplementary material available at https://doi.org/10.1038/s41586-025-08947-7.

Correspondence and requests for materials should be addressed to Junbiao Dai or Hongzhi Tang.

Peer review information *Nature* thanks the anonymous reviewers for their contribution to the peer review of this work. Peer reviewer reports are available.

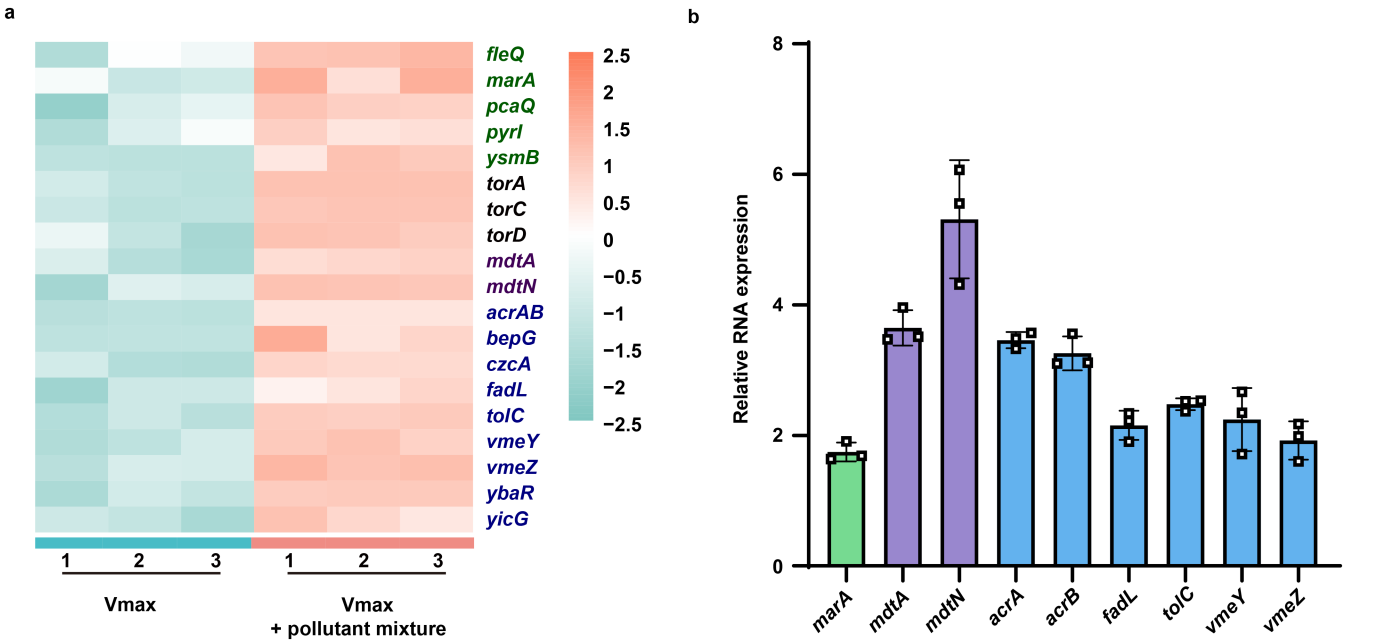

Extended Data Fig. 1 | Comparative transcriptomic analysis of *Vibrio natriegens* Vmax in the presence and absence of complex organic pollutants. **a**, Heatmap of differentially expressed genes related to aromatic compound resistance, detected based on RNA-seq of *V. natriegens* Vmax in the presence or absence of the indicated mixture of complex organic pollutants. Transcription factors are in green; energy metabolism genes are in black; multidrug-resistance-related genes are in purple; ABC transporter genes are in blue. **b**, qPCR analysis of expression of the indicated genes. Data are represented as the mean of three biological triplicates ± SD.

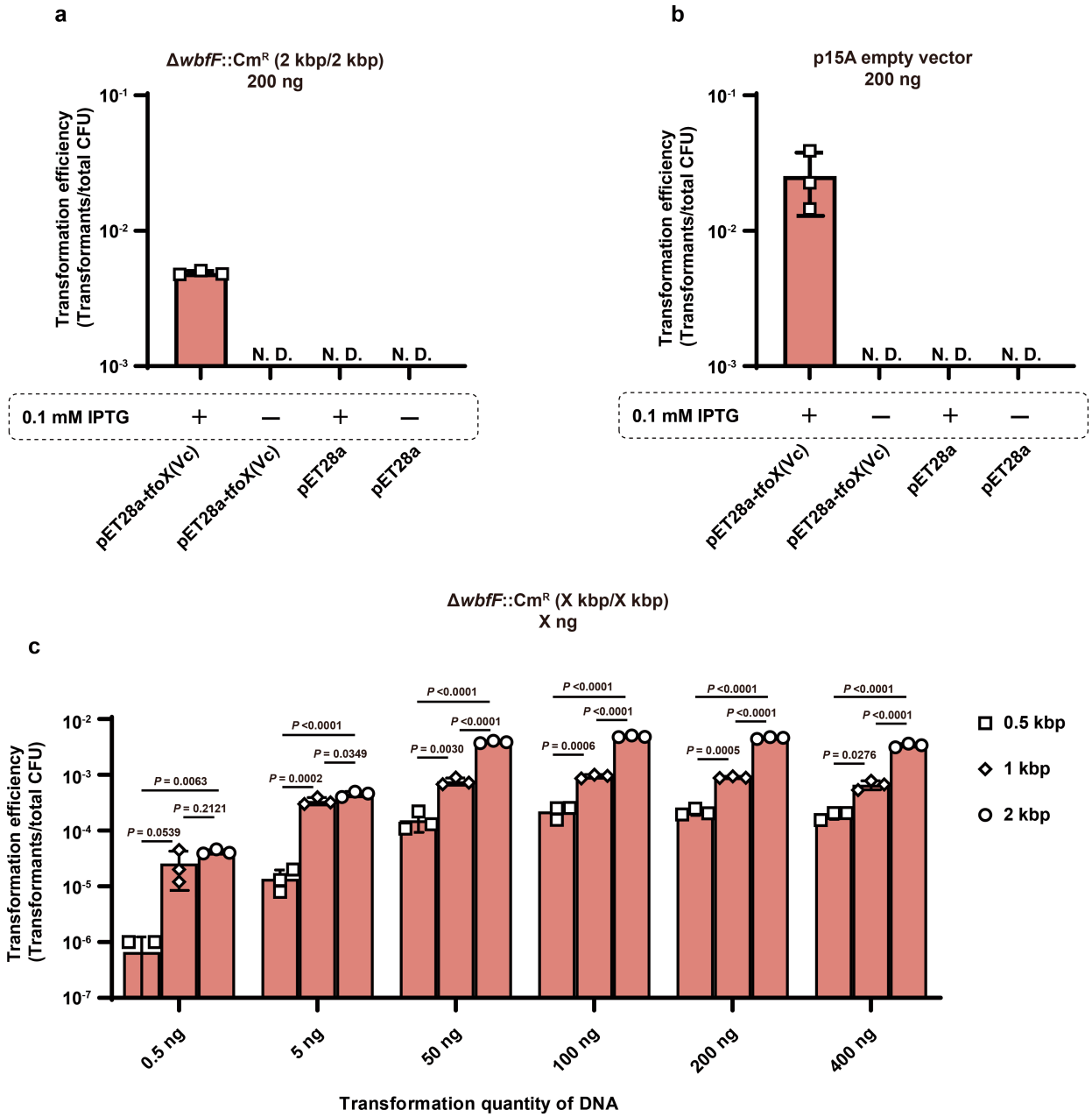

Extended Data Fig. 2 | Natural transformation (NT) efficiency of VCOD-1 (Vmax-pET28a-*tfoX*). **a**, NT efficiency testing between VCOD-1 and the original strain with a linear fragment (xxxx) as the donor. **b**, NT efficiency testing between VCOD-1 and the original strain with the p15A plasmid. **c**. NT efficiency of VCOD-1 with the indicated quantity of the Δ*wbfF*::*Cm*^{R} donor DNA fragment containing the indicated length (in kbp) of homology arms on each side of the mutation. Statistical analysis: **a**-**c**, data are represented as the mean ± SD. n = 3 independent experiments. Statistical significance was assessed using one-way ANOVA with Tukey's multiple comparisons tests.

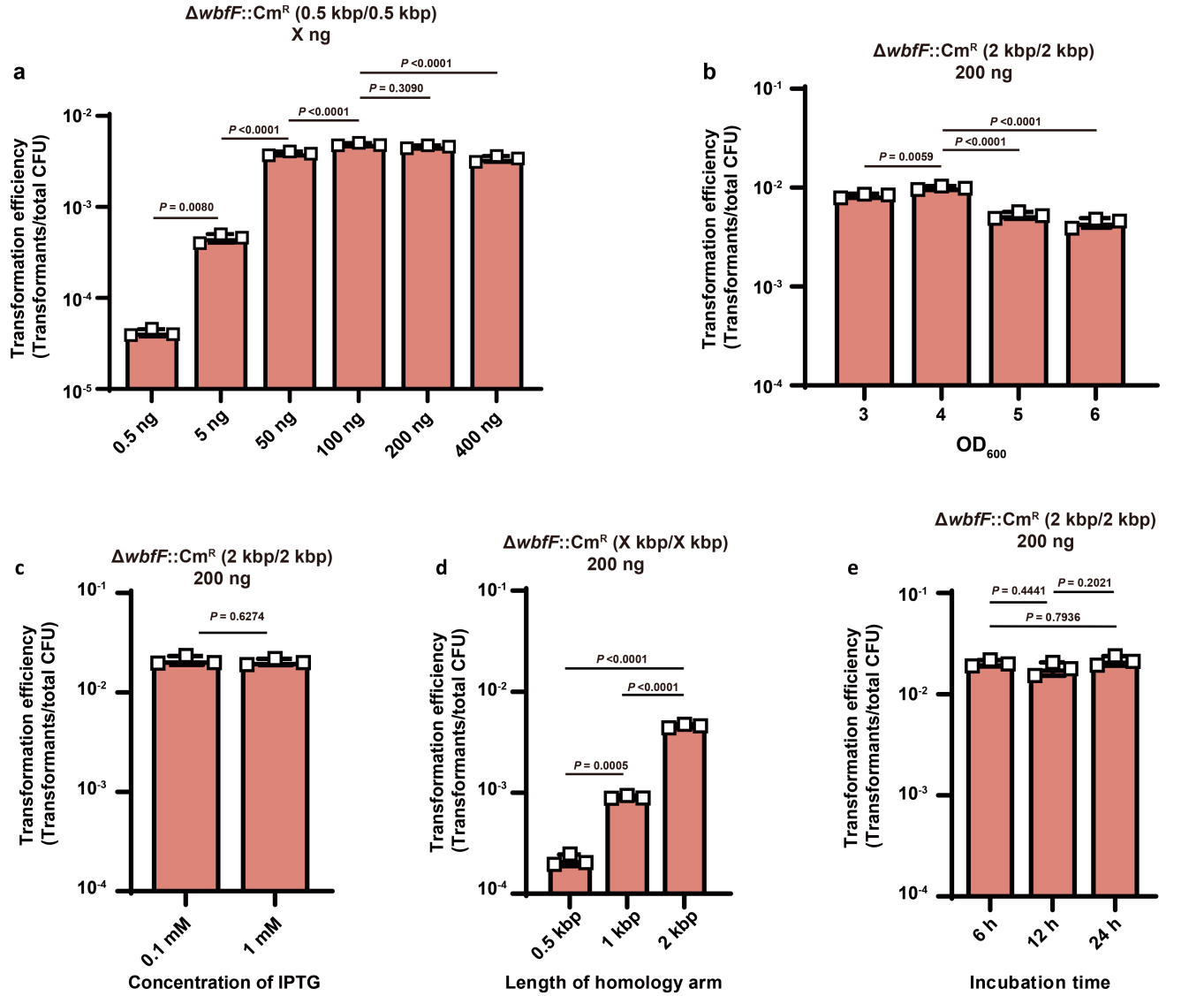

Extended Data Fig. 3 | Optimization of NT for VCOD-2 (VmaxΔ*int*::*tfoX*). **a**, NT efficiency of VCOD-2 with the indicated quantities of the Δ*wbfF*::*Cm*^{R} donor DNA fragment (with 0.5 kbp/0.5 kbp homology arms). **b**, NT efficiency of VCOD-2 in the indicated bacterial growth states (measured by OD_{600}) with 200 ng Δ*wbfF*::*Cm*^{R} (with 2 kbp/2 kbp homology arms) of the donor DNA fragment. **c**, NT efficiency of VCOD-2 induced by the indicated concentrations of IPTG with 200 ng of the Δ*wbfF*::*Cm*^{R} (2 kbp/2 kbp) donor DNA fragment. **d**, NT efficiency of VCOD-2 with 200 ng of the Δ*wbfF*::*Cm*^{R} donor DNA fragment (containing the indicated lengths for homology arms). **e**, NT efficiency of VCOD-2 with different incubation times after adding 200 ng of the Δ*wbfF*::*Cm*^{R} (2 kbp/2 kbp) donor DNA fragment. Statistical analysis: **a**-**e**, data are represented as the mean ± SD. n = 3 independent experiments. Statistical significance was assessed using one-way ANOVA with Tukey's multiple comparisons tests.

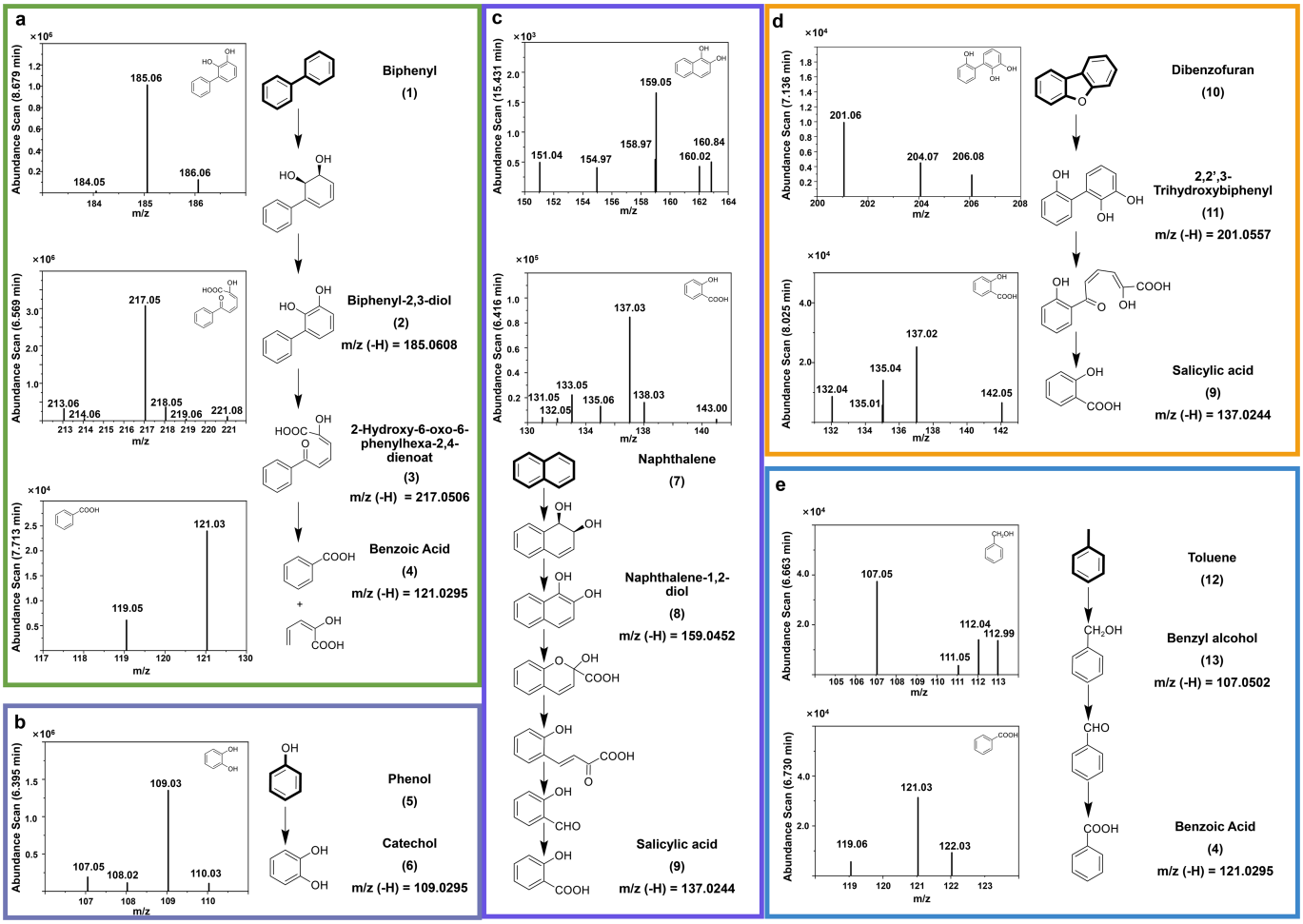

Extended Data Fig. 4 | Pathways for complex pollutant degradation by Vmax engineered strains. a-e, Catabolic pathways and LC-MS spectra for degradation intermediates produced by the VCOD-3 (**a**), VCOD-4 (**b**), VCOD-5 (**c**), VCOD-6 (**d**), and VCOD-7 (**e**) strains. The organic pollutants were added to resting cell suspensions in nine-salt solution (see Supplementary Information Table 2 for the detailed composition); metabolites were extracted by ethyl acetate after six-hour incubation of cultures with the pollutants (see Methods and Materials for details). Detected biphenyl degradation intermediates included: biphenyl-2,3-diol (**2**), 2-hydroxy-6-oxo-6-phenylhexa-2,4-dienoate (**3**), and benzoic acid (**4**). Catechol was detected as a phenol degradation intermediate (**6**). Detected naphthalene degradation intermediates included naphthalene-1,2-diol (8) and salicylic acid (**9**). Detected dibenzofuran degradation intermediates included 2,2',3-trihydroxybiphenyl (**11**) and salicylic acid (**9**). Detected toluene degradation intermediates included benzyl alcohol (**13**) and benzoic acid (**4**).

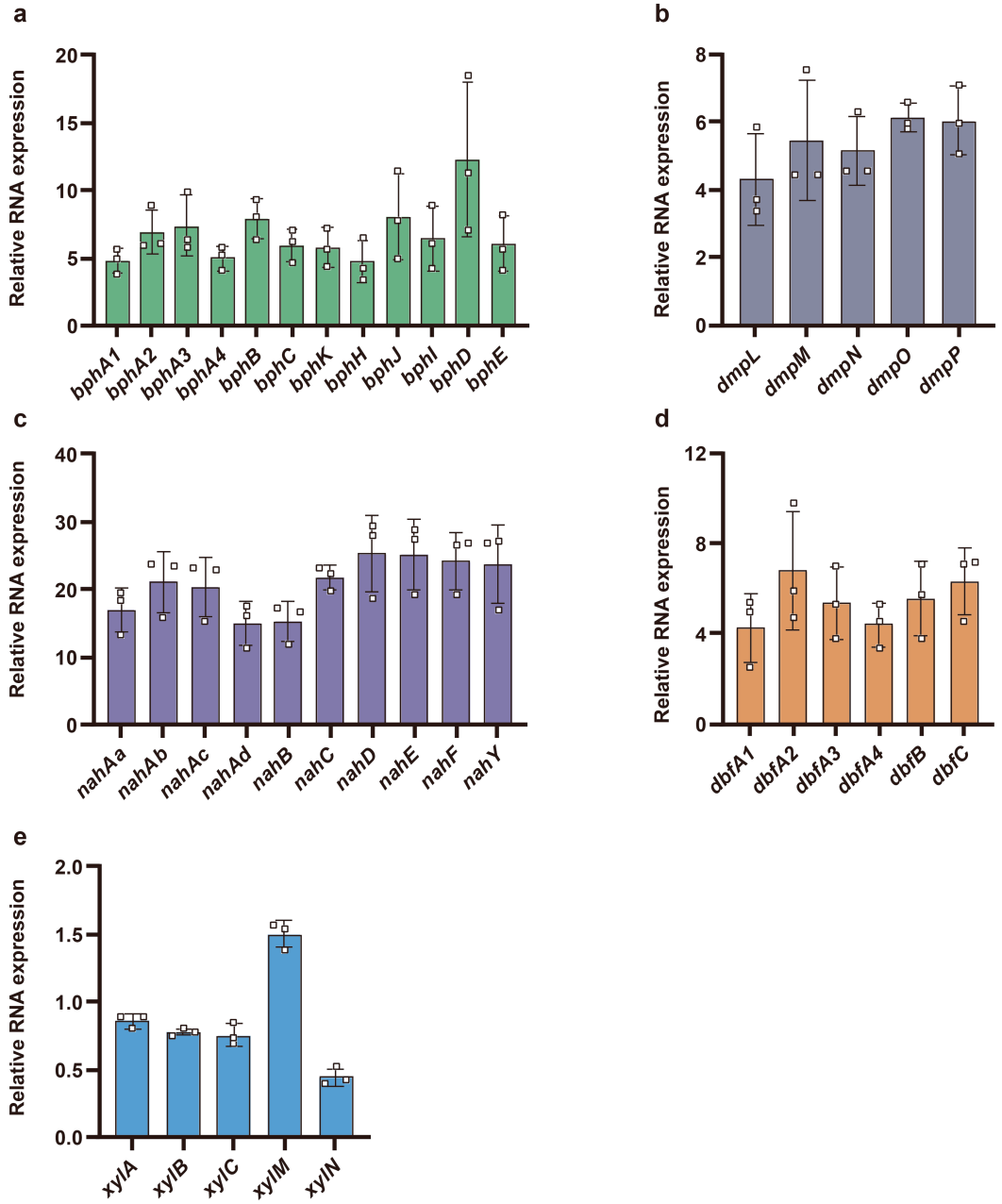

Extended Data Fig. 5 | qPCR analysis of selected analyte genes from the complex pollutant degrading gene clusters. a-e, Cultures of all strains were induced using 1 mM IPTG. The analyte genes (as indicated) were assessed with qPCR for strains VCOD-3 (**a**), VCOD-4 (**b**), VCOD-5 (**c**), VCOD-6 (**d**), and VCOD-7 (**e**) strains. Data are represented as the mean ± SD. n = 3 independent experiments.

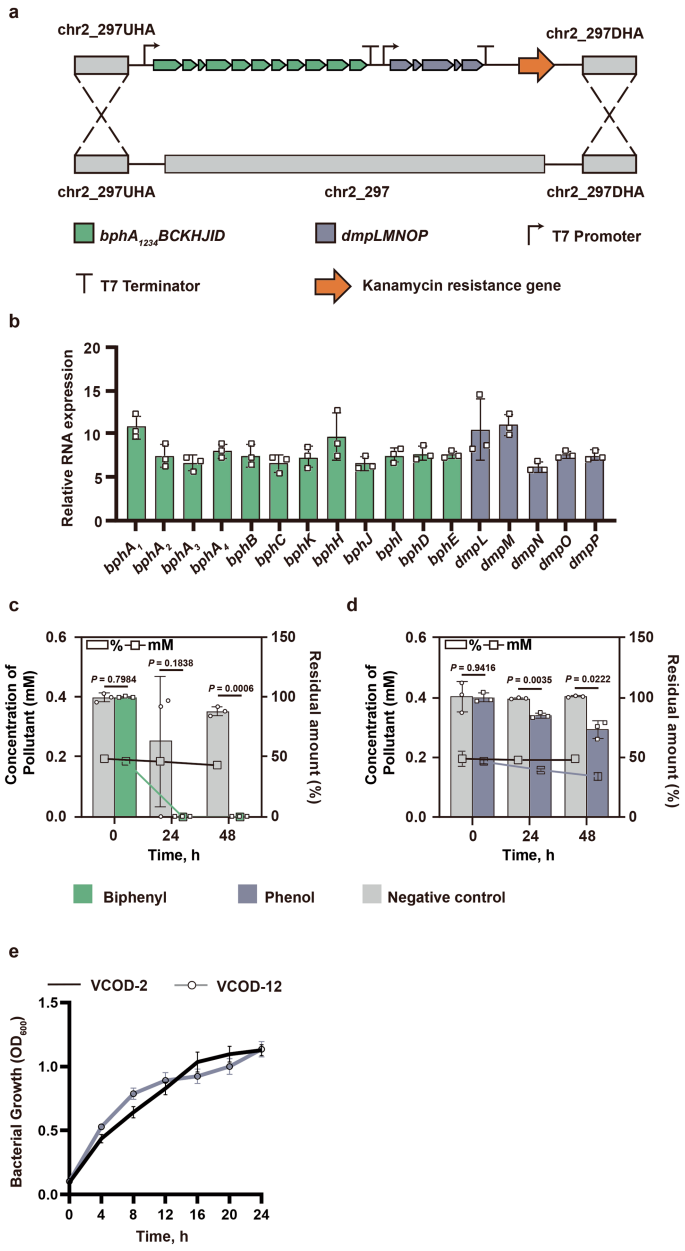

Extended Data Fig. 6 | Examining the remediation of complex organic pollutants by VCOD-12 and expression analysis of selected genes. **a**, Schematic for the organization of gene clusters in VCOD-12. Two gene clusters were inserted into the neutral site chr2_297. The screening marker kanamycin resistance gene *KanR* was present at the end of the *dmp* gene cluster. **b**, qPCR analysis of the indicated genes from the complex pollutant degrading gene cluster in VCOD-12, induced with 1 mM IPTG. **c**-**d**, Complex organic pollutant remediation efficiency of VCOD-12 in nine-salt solution. **e**, Growth of the VCOD-2 and VCOD-12 strains in LB_3 medium. Statistical analysis: **b**-**e**, data are represented as the mean ± SD. n = 3 independent experiments. Statistical significance was assessed using unpaired *t*-tests with Welch's correction.

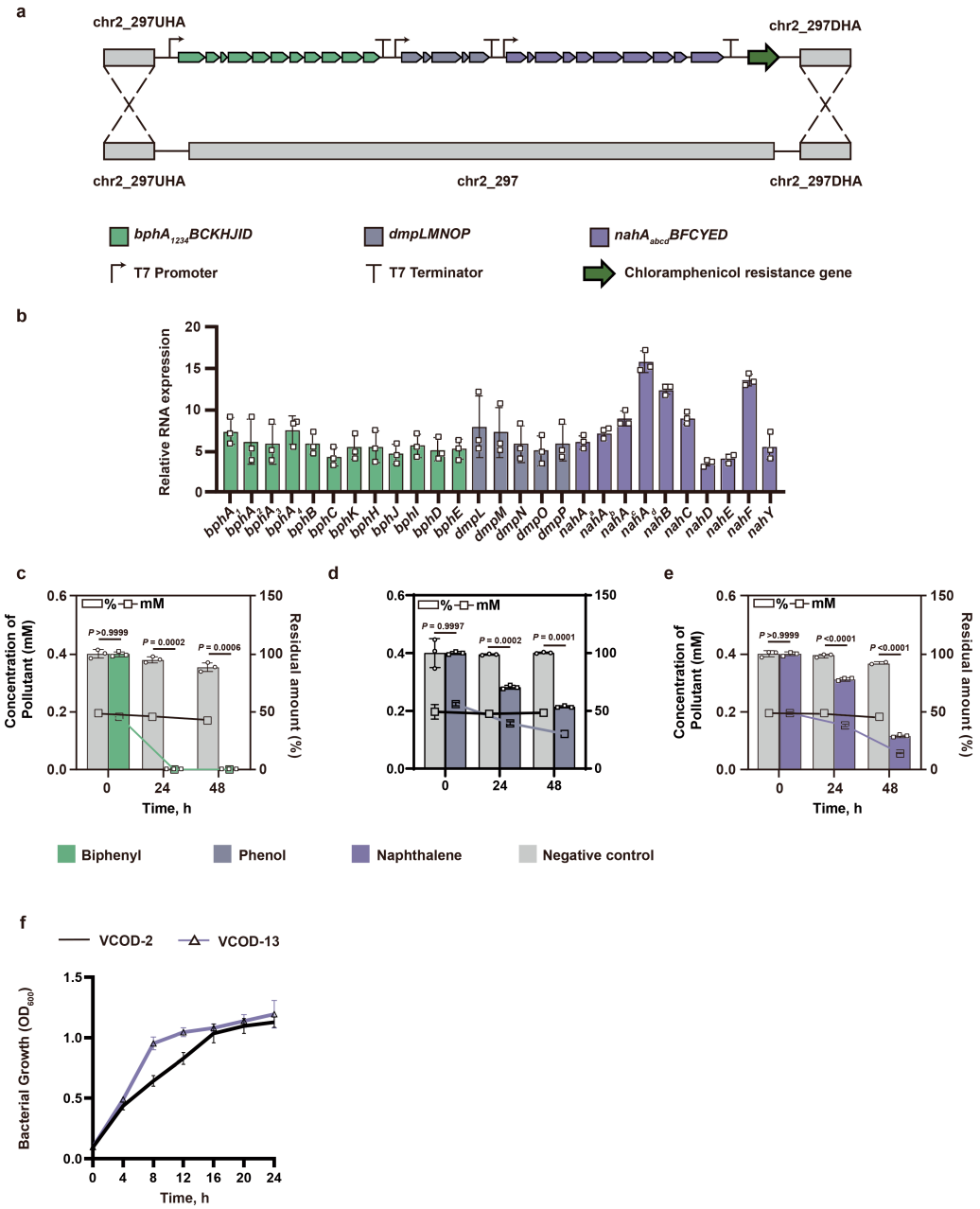

Extended Data Fig. 7 | Examining the remediation of complex organic pollutants by VCOD-13 and expression analysis for selected genes. **a**, Schematic for the organization of gene clusters in VCOD-13. Three gene clusters were inserted into the neutral site chr2_297. The screening marker chloramphenicol resistance gene Cm^R was present at the end of the *nah* gene cluster. **b**, qPCR analysis of the indicated genes from the complex pollutant degrading gene cluster in VCOD-13, induced with 1 mM IPTG. **c-e**, Complex organic pollutant remediation efficiency of VCOD-13 in nine-salt solution. **f**, Growth of the VCOD-2 and VCOD-13 strains in LB_3 medium. Statistical analysis: **b-f**, data are represented as the mean ± SD. n = 3 independent experiments. Statistical significance was assessed using unpaired *t*-tests with Welch's correction.

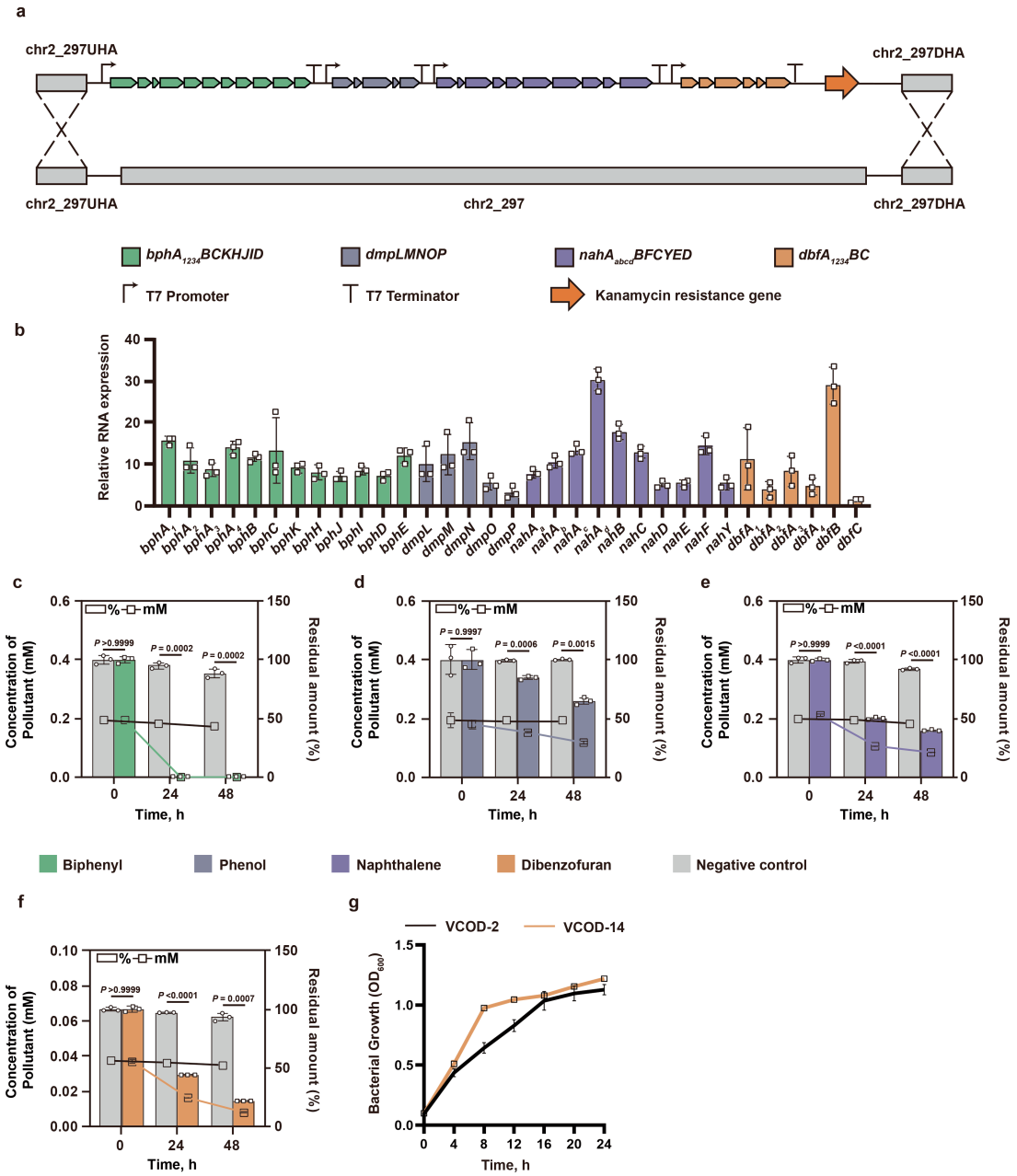

Extended Data Fig. 8 | Examining the remediation of complex organic pollutants by VCOD-14 and gene expression levels. a, Schematic for the organization of gene clusters in VCOD-14. Four gene clusters were inserted into the neutral site chr2_297. The screening marker kanamycin resistance gene *KanR* was present at the end of the *nah* gene cluster. **b**, qPCR analysis of the indicated genes from the complex pollutant degrading gene cluster in transformed *V. natriegens* cultures, induced with 1 mM IPTG. **c-f**, Complex organic pollutant remediation efficiency of VCOD-14 in nine-salt solution. **g**, Bacterial growth of strains VCOD-2 and VCOD-14 in LB_3 medium. Statistical analysis: **b-g**, data are represented as the mean ± SD. n = 3 independent experiments. Statistical significance was assessed using unpaired *t*-test with Welch's correction.

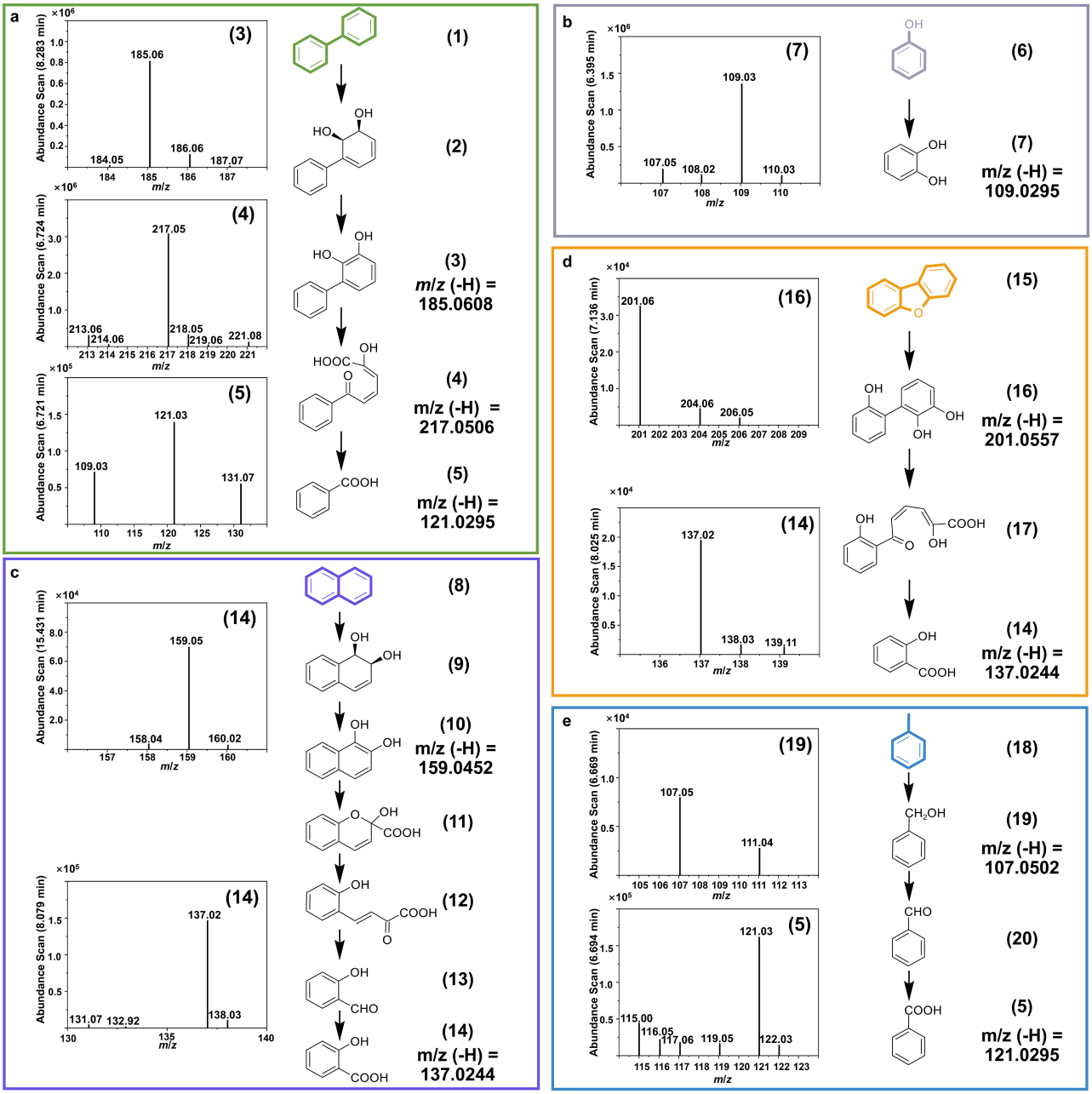

Extended Data Fig. 9 | Pathways for complex pollutant degradation by VCOD-15. a-e, Catabolic pathways and LC-MS spectra for degradation intermediates of biphenyl (**1**) (**a**), phenol (**6**) (**b**), naphthalene (**8**) (**c**), dibenzofuran (**15**) (**d**), and toluene (**18**) (**e**). The organic pollutants were added to resting cell suspensions in nine-salt solution; metabolites were extracted by ethyl acetate after six hours (see Methods and Materials for details). Detected biphenyl degradation intermediates included biphenyl-2,3-diol (**3**), 2-hydroxy-6-oxo-6-phenylhexa-2,4-dienoate (**4**), and benzoic acid (**5**). Catechol was a detected degradation intermediate from phenol (**7**). Detected naphthalene degradation intermediates included naphthalene-1,2-diol (**10**) and salicylic acid (**14**). Detected dibenzofuran degradation intermediates included 2,2′,3-trihydroxybiphenyl (**16**) and salicylic acid (**14**). Detected toluene degradation intermediates included benzyl alcohol (**19**) and benzoic acid (**5**).

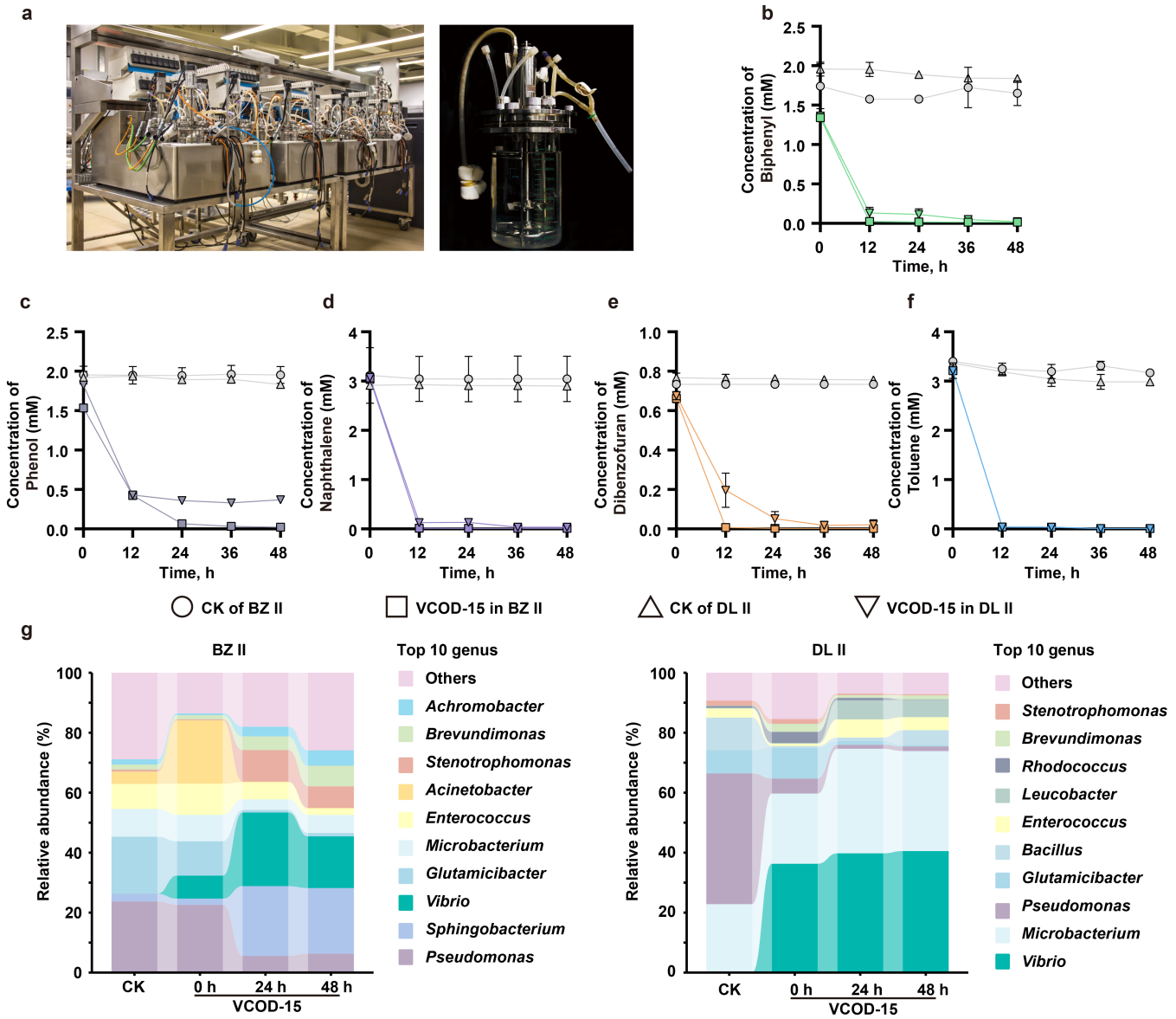

Extended Data Fig. 10 | Bioremediation of industrial wastewater samples in multi-parallel bioreactors. a, Photograph of the multi-parallel bioreactors. Industrial wastewater samples were treated with VCOD-15. **b-f**, Complex organic pollutant bioremediation efficiency of VCOD-15 in industrial wastewater samples. **g**, The relative abundance of microbial genera in the wastewater samples' microbial communities was measured at 0, 24, and 48 h during the bioremediation process (n = 3). **b-f**, Data are represented as the mean of three biological triplicates ± SD.

nature portfolio

Corresponding author(s): Hongzhi Tang, Junbiao Dai

Last updated by author(s): Mar 5, 2025

Reporting Summary

Nature Portfolio wishes to improve the reproducibility of the work that we publish. This form provides structure for consistency and transparency in reporting. For further information on Nature Portfolio policies, see our Editorial Policies and the Editorial Policy Checklist.

Statistics

For all statistical analyses, confirm that the following items are present in the figure legend, table legend, main text, or Methods section.

n/a	Confirmed
☐	☒ The exact sample size (*n*) for each experimental group/condition, given as a discrete number and unit of measurement
☐	☒ A statement on whether measurements were taken from distinct samples or whether the same sample was measured repeatedly
☐	☒ The statistical test(s) used AND whether they are one- or two-sided *Only common tests should be described solely by name; describe more complex techniques in the Methods section.*
☒	☐ A description of all covariates tested
☐	☒ A description of any assumptions or corrections, such as tests of normality and adjustment for multiple comparisons
☐	☒ A full description of the statistical parameters including central tendency (e.g. means) or other basic estimates (e.g. regression coefficient) AND variation (e.g. standard deviation) or associated estimates of uncertainty (e.g. confidence intervals)
☐	☒ For null hypothesis testing, the test statistic (e.g. *F*, *t*, *r*) with confidence intervals, effect sizes, degrees of freedom and *P* value noted *Give P values as exact values whenever suitable.*
☒	☐ For Bayesian analysis, information on the choice of priors and Markov chain Monte Carlo settings
☒	☐ For hierarchical and complex designs, identification of the appropriate level for tests and full reporting of outcomes
☒	☐ Estimates of effect sizes (e.g. Cohen's *d*, Pearson's *r*), indicating how they were calculated

Our web collection on statistics for biologists contains articles on many of the points above.

Software and code

Policy information about availability of computer code

Data collection	i-control and BioScreen PRO SW (BioScreener) was used to collect the data generated by microplate reader, including OD600 and fluorescence absorption. Agilent ChemStation B. 03. 02 and Agilent Openlab CDS 2.0 were used to collect the data generated by HPLC. Agilent MassHunter B. 07. 00 was used to collect the LC/MS data. Thermo Scientific Xcalibur (version 4.2.47) Data System was used for HRGC-MS data collection.
Data analysis	Microsoft Excel (Office 365) , Graphpad Prism 8.0 and Origin 2023 were used to analyze data.

For manuscripts utilizing custom algorithms or software that are central to the research but not yet described in published literature, software must be made available to editors and reviewers. We strongly encourage code deposition in a community repository (e.g. GitHub). See the Nature Portfolio guidelines for submitting code & software for further information.

Data

Policy information about availability of data

All manuscripts must include a data availability statement. This statement should provide the following information, where applicable:

- Accession codes, unique identifiers, or web links for publicly available datasets
- A description of any restrictions on data availability
- For clinical datasets or third party data, please ensure that the statement adheres to our policy

A reporting summary for this article is available as Supplementary Information file. Genome assembly generated in this study have been deposited into NCBI under the Bioproject PRJNA1240198. All other data are presented in the paper and associated supplementary materials. Source data are provided in this paper. Public data used in this study include function annotations of non-essential genes in the genome of Vmax and degradation gene clusters from the NCBI database (https://www.ncbi.nlm.nih.gov), and the accession numbers of the genes are listed in Supplementary Tables 4 and 5.

Research involving human participants, their data, or biological material

Policy information about studies with human participants or human data. See also policy information about sex, gender (identity/presentation), and sexual orientation and race, ethnicity and racism.

Reporting on sex and gender	There is no experiment or other research activity associated with human participants or human data. So there is no reporting on sex or gender.
Reporting on race, ethnicity, or other socially relevant groupings	There is no experiment or other research activity associated with human participants or human data. So there is no reporting on race, ethnicity, or other socially relevant groupings.
Population characteristics	There is no experiment or other research activity associated with human participants or human data. So there is no reporting or announcement on population characteristics.
Recruitment	There is no experiment or other research activity associated with human participants or human data. So there is no reporting on recruitment.
Ethics oversight	There is no experiment or other research activity associated with human participants or human data. So there is no reporting on ethics oversights.

Note that full information on the approval of the study protocol must also be provided in the manuscript.

Field-specific reporting

Please select the one below that is the best fit for your research. If you are not sure, read the appropriate sections before making your selection.

☒ Life sciences ☐ Behavioural & social sciences ☐ Ecological, evolutionary & environmental sciences

For a reference copy of the document with all sections, see nature.com/documents/nr-reporting-summary-flat.pdf

Life sciences study design

All studies must disclose on these points even when the disclosure is negative.

Sample size	No statistical methods were used to predetermine sample size. Experiments were performed in biological triplicate n=3 unless otherwise noted.
Data exclusions	No data were excluded from the analyses.
Replication	All attempts at replication were successful.
Randomization	Because there were no need to allocate samples into experimental groups in essence, this is not relevant to our study.
Blinding	Because there were no need to allocate samples into experimental groups in essence, this is not relevant to our study.

Reporting for specific materials, systems and methods

We require information from authors about some types of materials, experimental systems and methods used in many studies. Here, indicate whether each material, system or method listed is relevant to your study. If you are not sure if a list item applies to your research, read the appropriate section before selecting a response.

Materials & experimental systems

n/a	Involved in the study
☒	☐ Antibodies
☒	☐ Eukaryotic cell lines
☒	☐ Palaeontology and archaeology
☒	☐ Animals and other organisms
☒	☐ Clinical data
☒	☐ Dual use research of concern
☒	☐ Plants

Methods

n/a	Involved in the study
☒	☐ ChIP-seq
☒	☐ Flow cytometry
☒	☐ MRI-based neuroimaging

Plants

Seed stocks	No seed stocks of plants were involved in this study.
Novel plant genotypes	No plants with novel genotypes were involved in this study.
Authentication	No authentication procedues were involved in this study.